IEEE Access
Multidisciplinary ⋮ Rapid Review ⋮ Open Access Journal

Received 9 June 2024, accepted 2 July 2024, date of publication 9 July 2024, date of current version 18 July 2024.

Digital Object Identifier 10.1109/ACCESS.2024.3425441

RESEARCH ARTICLE

Configuration Synthesis of Fully-Symmetrical Parallel Positioning Mechanism for In Situ Machining of Large Structural Components

YANG QI[1], XINQI TAO[1], XIAOFEI REN[2], AND HONG WANG[1]
[1]School of Mechanical Engineering, Tianjin University of Technology and Education, Tianjin 300222, China
[2]Office of Academic Affairs, Tianjin University of Technology and Education, Tianjin 300222, China

Corresponding author: Yang Qi (qiyang@tju.edu.cn)

This work was supported in part by Tianjin Science and Technology Plan Project 22JCYBJC01670 and Project 21JCZDJC00820, and in part by Tianjin University Science and Technology Development Fund under Project 2020KJ105.

ABSTRACT The surface of large structural components is composed of materials with different hardness and complex shapes, and it presents significant challenges in achieving precise and efficient positioning as well as high-precision grinding. In-situ processing machine overcomes the limitations of grinding machines such as poor adaptability to different materials and limited travel, and becomes a promising solution for efficient processing of large complex structural components. In-situ processing machine is composed of car, positioning and different processing devices. The positioning mechanism with full-symmetrical layout in parallel topology can effectively guarantee the positioning accuracy and machining stiffness, and is the best scheme for in-situ machining mechanism. Aiming to provide a novel topology structure for subsequent mechanism development. This paper carries out theoretical research on the composition of its topological structure. As an efficient configuration synthesis theory combining numerical and geometrical aspects, finite and instantaneous screw (FIS) theory is applied in this paper. Firstly, the required motions for the grinding operation are characterized based on finite screw, representing the desired motion of the mechanism. Then, single-degree-of-freedom factors are added afterwards to obtain the standard type of the limb structure. Secondly, the factors in the standard type are equivalent transformations and displacements based on the properties of screw triangle product to obtain the derivative and expanded types of limb structure. The feasibility is verified through the synthesis algorithm or transformation properties of finite screw. Finally, taking three feasible limb structures as examples, three fully-symmetrical parallel positioning mechanisms are configured based on assembly conditions and actual requirements. This paper presents a configuration synthesis process for the fully-symmetrical parallel positioning mechanism, obtaining various new topology structures and laying a theoretical foundation for subsequent research.

INDEX TERMS Configuration synthesis, in-situ machining, FIS theory.

I. INTRODUCTION

High-end equipment in aerospace, new energy and other fields continues to emerge. Large core components with dimensions ranging from tens of meters to hundreds of meters, such as spacecraft shells and wind turbine blades, involve multiple processes in the manufacturing process. The processing quality of the grinding process determines the reliability and adaptability of the equipment. There are currently three methods for processing such components. Method 1 is to perform partial manual operations on the processing part. Method 2 is to disassemble and group the components before move them to CNC machine tools for grinding operations. After the processing is completed, the components are reassembled. Method 3 combines robot technology to achieve in-situ grinding of components without

The associate editor coordinating the review of this manuscript and approving it for publication was Guilin Yang.

moving the workpiece, by using a robot with a mobile device. Method 1 has low efficiency, and the precision of manual operation is difficult to meet the required accuracy of the components, resulting in poor processing quality. Method 2 by machining with machine tools, can guarantee a certain level of precision. However, the machining stroke of the CNC machine tools available on the market currently cannot meet the requirements for ultra-long-sized components, necessitating step-by-step processing. During this process, various factors such as force and temperature can impact and result in residual stress, leading to inaccurate machining. Compared to the other two methods, Method 3 is more flexible and has significant advantages in terms of machining rigidity and precision through robot operation. The workpiece does not need to be disassembled, only fixed in place. The mobile device carries the robot, allowing it to move extensively around the workpiece. Once it reaches the desired processing area, the robot locks onto the machining zone and starts the grinding operation, achieving in-situ processing.

Currently, in-situ grinding robots can be classified into series and parallel structures, both capable of performing grinding operations. Researchers such as Chen et al. [1] designed a robot based on a series structure for grinding processes, which has shown a 19.2% reduction in surface roughness of components and improved the quality of the component surface after grinding operations. Li et al. [2] adopted a serial robot with six Degrees of Freedom (DoF) to perform grinding processing on large aerospace engine blades in the field of space exploration. Compared to manual work, the serial robot better ensures the contour quality of the blades after grinding operations. Wang et al. [3] derived a dynamic model of a six-joint serial robot using the Bouc-Wen model, enabling better control of the force applied when the robot interacts with components during grinding operations. Serial robots have demonstrated high efficiency and flexibility in the grinding process, overcoming the limitations of the stroke in traditional machines and the low efficiency of manual operations on assembly lines. However, the stiffness and precision of multi-joint robots with a serial structure are relatively low, making it prone to positional deviations and inaccurate positioning during the grinding of large components. Due to the series composition of all joints, their load capacity is weaker compared to parallel mechanisms. Guo et al. [4] designed a 5-DoF polishing hybrid robot by combining a high-precision and compact parallel structure with a serial structure. This design improves the grinding capability for components with complex surface profiles. Feng et al. [5] combined a 6-UPS parallel mechanism with a four-joint serial mechanism to design a hybrid processing robot for large components. They achieved the processing operations on the components by driving the parallel mechanism to control the serial manipulator mounted on its moving platform. Xu et al. [6] designed a hybrid robot for machining the internal cavities of large components by combining a 4-DoF 2RRU-RRS parallel mechanism with a 2-DoF serial mechanism. They utilized the advantages of specific rotation axes to efficiently perform machining operations in areas that are difficult for manual processing. Compared to multi-joint robots with series structures, hybrid robots improve overall rigidity and precision. However, hybrid robots have a smaller workspace and are prone to coupling effects. The combination of parallel and serial structures also adds complexity to robot control.

To address the aforementioned issue, Xie et al. [7] utilized a coupled parallel pose adjustment mechanism as the processing machine to accomplish milling, hole-making, and polishing for large components. Olarra et al. [8] developed the WalkingHex parallel mechanism as a miniature machine tool capable of precisely milling large structural components with complex surface shapes. Chen et al. [9] adopted the in-situ processing mode for large steel components and used parallel mechanisms to achieve the precise processing requirements for steel components. Parallel mechanisms, as processing machine tools, demonstrate their capabilities in various machining operations on large structural components. Considering the stiffness and precision of in-situ grinding robot, a compact full-symmetric parallel mechanism with high stiffness is adopted for grinding operation. The use of identical and symmetrical supporting limbs increases the overall stiffness of the mechanism. During the grinding process, it is important to fully engage with every surface of the workpiece. However, multi-joint serial structures are prone to inaccurate displacement positioning during operation. Therefore, a three-translational (3T) parallel mechanism is adopted to achieve precise positioning. When in-situ grinding robots are faced with large components with complex surface structures, constant adjustment of the end effector's orientation is needed to adapt to the grinding operations on different curved surfaces. To achieve excellent orientation adjustment capability, an additional rotational motion (1R) needs to be integrated into the mechanism. Based on this, it is indeed necessary to carry out configuration synthesis for a 4-DoF fully-symmetrical parallel mechanism with three translational movements and one rotational movement (3T1R) for precise positioning.

The methods of configuration synthesis of mechanisms include constrained screw synthesis method, displacement manifold synthesis method, differential geometry synthesis method and orientation feature method [10], [11], [12], [13]. The above configuration methods need to consider the full cycle of the mechanism or rely on experience to solve algebraic operations when synthesizing the mechanism. In order to solve the issue present in existing methods, it is particularly important to accurately derive the relevant operations and unify the finite motion of the mechanism, support chain and joint. The finite and instantaneous screw (FIS) theory can unify the topological and parametric models under the framework of screw theory [14], [15], [16]. Based on the finite screw, the expression of the finite motion between the joint and the limb or between the limb and the moving platform can be established. Yang et al. Yang et al. proved that algebraic synthesis at a finite motion level does not require

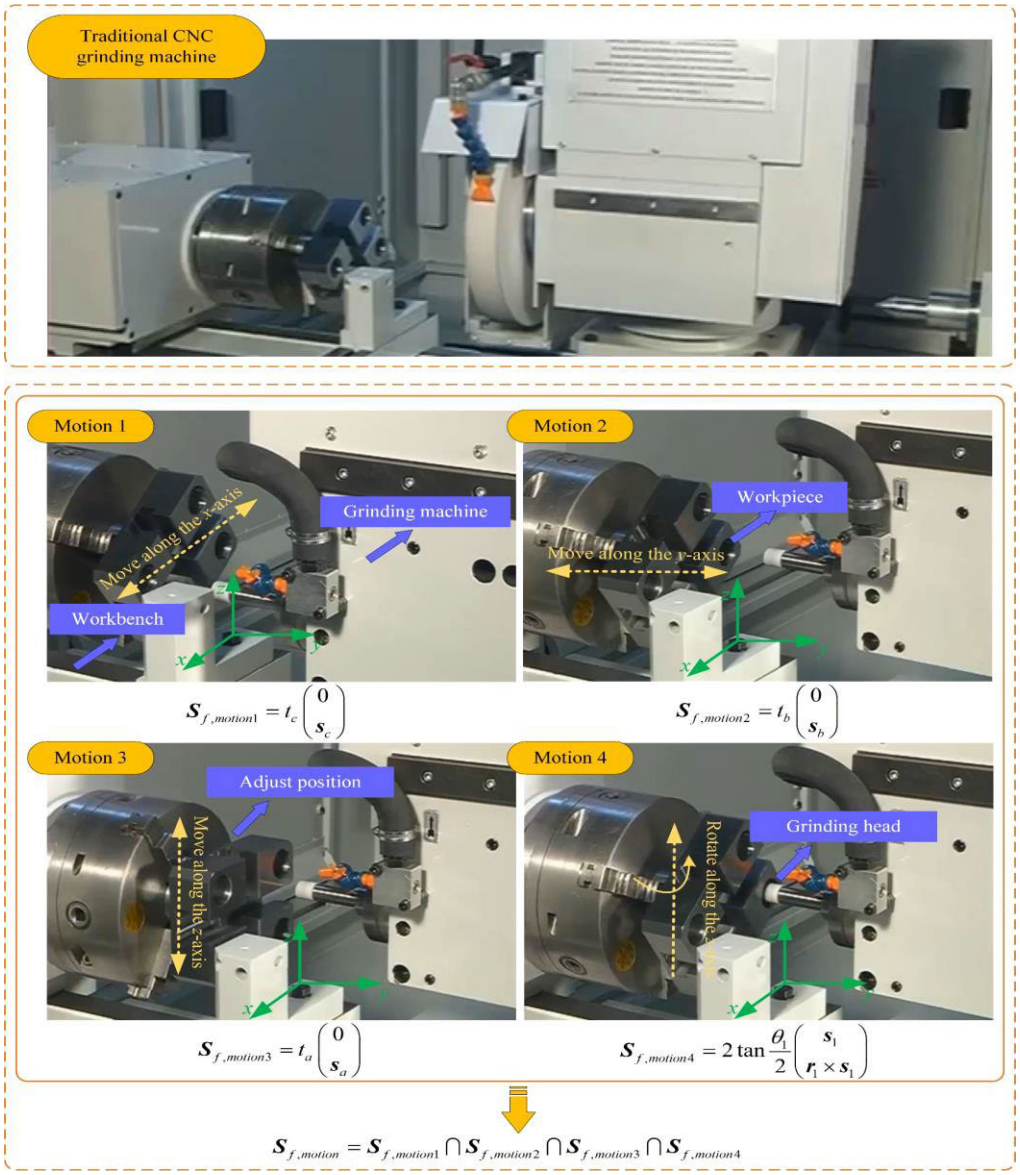

FIGURE 1. The grinding motion of a CNC grinder.

verification of the full cycle degree of freedom of the parallel mechanism synthesized by the configuration [17]. A variety of parallel mechanisms with three translational motions are constructed by the finite screw method. Sun et al. [18] used this method to construct a variety of parallel mechanisms with 2R1T. This method can clearly characterize the finite motion and has accurate operation criteria. However, this method has not been applied to the configuration synthesis of 3T1R parallel mechanisms. Therefore, it is necessary to propose a synthesis procedure for the configuration of 3T1R parallel mechanisms.

This paper conducts a configuration synthesis of 3T1R parallel mechanism based on the finite and instantaneous screw (FIS) theory. Firstly, the analytical expression of the mechanism's grinding motion is represented based on finite screw, leading to the determination of the initial configuration structure. Then, by introducing parameter factors to the initial structure, the standard Type I and Type II structures are obtained. Based on the standard Type I, II, equivalent derivations are performed to obtain derived Type I and expanded Type I and Type II structures. Finally, design the assembly conditions of the mechanism according to the actual operational requirements to obtain the 3T1R parallel mechanism. This study is of great significance for the configuration synthesis of grinding robots targeting large components.

II. INITIAL CONFIGURATION OF 3T1R TYPE BASED ON FINITE SCEW

Grinding processing typically requires four movements, including one main movement and three feed movements. In the CNC universal grinder, after accurately positioning the workpiece using the three feed movements, the main

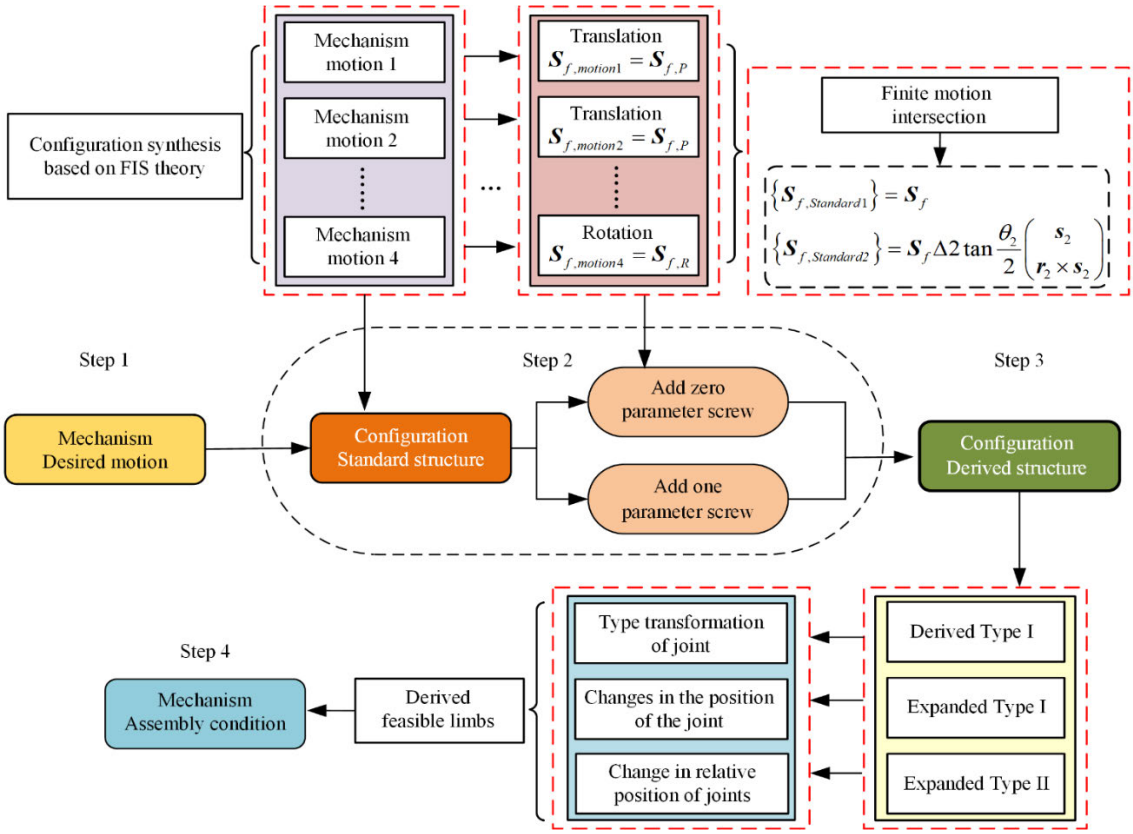

FIGURE 2. 3T1R configuration synthesis based on FIS theory.

movement is employed to carry out the grinding process on the workpiece, as shown in Fig. 1.

Therefore, in order to achieve grinding operations, a fully-symmetrical parallel mechanism for precise positioning needs to have at least three translational movements along different axes and one rotational movement around an axis. The x and y axes alter the flat position of the machined part, while the $z-axis$ adjusts the relative position between the tool and the part. The rotational movement is responsible for the grinding process. The desired motion of the initial configuration is 3T1R motion. The configuration synthesis is performed using FIS theory. The configuration process is illustrated in Fig. 2. Firstly, the initial configuration is represented by finite screws to characterize its continuous motion, which represents the desired motion of the mechanism. Secondly, adding 0 or 1 single-degree-of-freedom factor after the initial algebraic structure yields its standard form, denoted as Standard Type I and Standard Type II. Finally, the structures derived by equivalent joint transformations using the screw triangle product rule are designated as Derived Type I. By making specific joint position transformations or relative transformations within Derived Type I, new structures are obtained, denoted as Expanded Type I and Expanded Type II. Each of the Derived Type I and Expanded Type I and II structures is then verified for feasibility to obtain all feasible structures.

The FIS theory represents the joints of a mechanism using finite screws, which primarily consist of four elements: joint axis, rotation angle, position vector, and translation distance. The finite screw representations of commonly used revolute (R) and prismatic (P) joints are expressed as (1) and (2). The universal (U) and spherical (S) joints can be formed by combining two R joints with perpendicular axes and three R joints with axes intersecting at a point.

$$S_{f,R} = 2\tan\frac{\theta}{2}\begin{pmatrix} s \\ r \times s \end{pmatrix} \tag{1}$$

where $S_{f,R}$ represents the finite screw representation of an R joint, s and r denote the axis and position vector of the R joint respectively, and θ represents the angle rotated by the R joint during its motion.

$$S_{f,P} = t\begin{pmatrix} 0 \\ s \end{pmatrix} \tag{2}$$

where $S_{f,P}$ represents the finite screw representation of an P joint, t represents the distance generated by the motion of the P joint.

The motion of the limbs in the mechanism can be obtained by performing screw triangular product operations on the joints within the limbs, as shown in (3). As a result, the overall continuous motion of the mechanism is given by the intersection of the motions of the individual limbs, as shown

in (4).

$$\boldsymbol{S}_{f,i} = \boldsymbol{S}_{f,joint\,1} \Delta \boldsymbol{S}_{f,joint\,2} \Delta \cdots \Delta \boldsymbol{S}_{f,joint\ n} \tag{3}$$

where $\boldsymbol{S}_{f,i}$ represents the finite motion synthesized from all the joints in the ith limb. $\boldsymbol{S}_{f,joint\ k}, k = 1, 2 \cdots n$ represents the joints within the limb.

$$\boldsymbol{S}_f = \boldsymbol{S}_{f,1} \cap \boldsymbol{S}_{f,2} \cap \cdots \cap \boldsymbol{S}_{f,n} \tag{4}$$

where $\boldsymbol{S}_f$ represents the overall continuous motion of the mechanism.

The continuous motion required for a parallel positioning mechanism consists of spatial three-dimensional translation and rotation. The mechanism translates in three dimensions to position itself at the processing location of the component. It then adjusts its orientation through rotational motion to precisely position itself on the specific operational surface of the component, allowing for grinding operations on the surface. Finite screw based on FIS theory can describe the required continuous motion of the mechanism. That is, it can represent the desired motion of the mechanism, as shown in (5).

$$\{\boldsymbol{S}_f\} = \boldsymbol{t}_c \begin{pmatrix} 0 \\ \boldsymbol{s}_c \end{pmatrix} \Delta \boldsymbol{t}_b \begin{pmatrix} 0 \\ \boldsymbol{s}_b \end{pmatrix} \Delta \boldsymbol{t}_a \begin{pmatrix} 0 \\ \boldsymbol{s}_a \end{pmatrix} \Delta 2 \tan \frac{\theta_1}{2} \begin{pmatrix} \boldsymbol{s}_1 \\ \boldsymbol{r}_1 \times \boldsymbol{s}_1 \end{pmatrix} \tag{5}$$

The expected motion $\{\boldsymbol{S}_f\}$ of the mechanism is synthesized by the intersection of the motions in each $\boldsymbol{S}_{f,i}$ of the mechanism, while $\boldsymbol{S}_{f,i}$ is synthesized by the screw triangle product in each $\boldsymbol{S}_{f,joint\ k}, k = 1, 2 \cdots n$. Thus, under the condition of satisfying $\{\boldsymbol{S}_f\} \subseteq \boldsymbol{S}_{f,i}$, all feasible limb structures that meet the motion requirements can be configured. By adding 0 or 1 single-degree-of-freedom independent factor at the end of the characterization formula of the desired motion mentioned above, the standard Type I ($R_1 P_a P_b P_c$) and Standard Type II ($R_1 R_2 P_a P_b P_c$) of the parallel positioning mechanism can be obtained. The finite motion representations of the standard Type I and Type II are shown in (6) and (7) respectively, while the joint distribution is shown in Fig. 3 and Fig. 4.

$$\begin{aligned} \{\boldsymbol{S}_{f,Standard1}\} = {} & \boldsymbol{t}_c \begin{pmatrix} 0 \\ \boldsymbol{s}_c \end{pmatrix} \Delta \boldsymbol{t}_b \begin{pmatrix} 0 \\ \boldsymbol{s}_b \end{pmatrix} \Delta \boldsymbol{t}_a \begin{pmatrix} 0 \\ \boldsymbol{s}_a \end{pmatrix} \\ & \times \Delta 2 \tan \frac{\theta_1}{2} \begin{pmatrix} \boldsymbol{s}_1 \\ \boldsymbol{r}_1 \times \boldsymbol{s}_1 \end{pmatrix} \end{aligned} \tag{6}$$

$$\begin{aligned} \{\boldsymbol{S}_{f,Standard2}\} = {} & \boldsymbol{t}_c \begin{pmatrix} 0 \\ \boldsymbol{s}_c \end{pmatrix} \Delta \boldsymbol{t}_b \begin{pmatrix} 0 \\ \boldsymbol{s}_b \end{pmatrix} \Delta \boldsymbol{t}_a \begin{pmatrix} 0 \\ \boldsymbol{s}_a \end{pmatrix} \\ & \Delta 2 \tan \frac{\theta_2}{2} \begin{pmatrix} \boldsymbol{s}_2 \\ \boldsymbol{r}_2 \times \boldsymbol{s}_2 \end{pmatrix} \Delta 2 \tan \frac{\theta_1}{2} \begin{pmatrix} \boldsymbol{s}_1 \\ \boldsymbol{r}_1 \times \boldsymbol{s}_1 \end{pmatrix} \end{aligned} \tag{7}$$

In the standard Type I ($R_1 P_a P_b P_c$) and Type II ($R_1 R_2 P_a P_b P_c$) configurations, $\boldsymbol{s}_c$, $\boldsymbol{s}_b$, and $\boldsymbol{s}_a$ are linearly independent vectors. By performing equivalent replacements of joints through directional or circular translational motion in the standard configuration, derived Type I configurations can be obtained. In addition, the principle of screw triangle product can be used to change the positional relationship between the R factor and the P factor in the structure. When the relative position of the R factor remains unchanged, the P factor is shifted to obtain an extended Type I. When the relative position of the R factor changes, the P factor is shifted to obtain the extended type II.

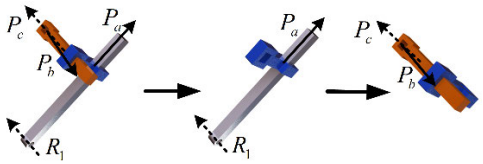

FIGURE 3. Joints of standard type I.

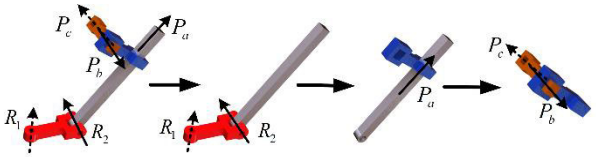

FIGURE 4. Joints of standard type II.

III. DERIVED AND EXPANDED TYPES OF THE STANDARD TYPE I CONFIGURATION

The standard Type I configuration is a 4-DOF limb structure. By performing equivalent replacements of joints in the standard Type I configuration, a derived Type I configuration with 4-DOF can be obtained. Two approaches can be taken, with the first involving the replacement of one P joint in the standard Type I configuration, i.e., $R_1 P_a \mapsto R_1 R_1$, resulting in the transformation of the standard Type I configuration into $R_1 R_1 P_b P_c$. Representing this structure using finite screw as in (8).

$$\begin{aligned} \{\boldsymbol{S'}_{f,4-\mathrm{DoF}}\}_{\mathrm{Derived\ I}} = {} & \boldsymbol{t}_c \begin{pmatrix} 0 \\ \boldsymbol{s}_c \end{pmatrix} \Delta \boldsymbol{t}_b \begin{pmatrix} 0 \\ \boldsymbol{s}_b \end{pmatrix} \\ & \times \Delta 2 \tan \frac{\theta_{12}}{2} \begin{pmatrix} \boldsymbol{s}_1 \\ \boldsymbol{r}_{12} \times \boldsymbol{s}_1 \end{pmatrix} \\ & \times \Delta 2 \tan \frac{\theta_{11}}{2} \begin{pmatrix} \boldsymbol{s}_1 \\ \boldsymbol{r}_{11} \times \boldsymbol{s}_1 \end{pmatrix} \end{aligned} \tag{8}$$

After the replacement of joints in the standard Type I configuration, the factors now contain two R joints with parallel axes. Using the composition algorithm of FIS theory, the R factors can be rewritten as a combination of circular translation and rotation, as shown in (9).

$$\begin{aligned} & \{\boldsymbol{S'}_{f,4-\mathrm{DoF}}\}_{\mathrm{Derived\ I}} \\ & = \boldsymbol{t}_c \begin{pmatrix} 0 \\ \boldsymbol{s}_c \end{pmatrix} \Delta \boldsymbol{t}_b \begin{pmatrix} 0 \\ \boldsymbol{s}_b \end{pmatrix} \\ & \quad \times \Delta \left(\left(\exp\left(-\theta_{12} \tilde{\boldsymbol{s}}_1\right) - \exp\left(- \sum_{i=1}^{2} \theta_{1i} \tilde{\boldsymbol{s}}_1 \right) \right) (\boldsymbol{r}_{12} - \boldsymbol{r}_{11}) \right) \end{aligned}$$

$$\times \Delta 2\tan\frac{\sum_{i=1}^{2}\theta_{1i}}{2}\begin{pmatrix}\boldsymbol{s}_1\\ \boldsymbol{r}_{12}\times\boldsymbol{s}_1\end{pmatrix} \tag{9}$$

where $\tilde{\boldsymbol{s}}_1$ is the skew-symmetric matrix of $\boldsymbol{s}_1$. When the two variables in the above equation are transformed by using (10), the third factor becomes a circle translation with a radius of $|\boldsymbol{r}_1-\boldsymbol{r}_{11}|$, which is equivalent to (6) under the conditions of $|\boldsymbol{r}_1-\boldsymbol{r}_{11}|\to\infty$ and $\boldsymbol{s}_1\times(\boldsymbol{s}_b\times\boldsymbol{s}_c)\neq 0$.

$$\sum_{i=1}^{2}\theta_{1i}\mapsto\theta_1,\boldsymbol{r}_{12}\mapsto\boldsymbol{r}_1 \tag{10}$$

The second involves replacing the two P joints in the standard Type I configuration, i.e., $R_1P_aP_b\mapsto R_1R_1R_1$. The standard Type I configuration is transformed into $R_1R_1R_1P_c$. Representing this structure using finite screw as in (11).

$$\begin{aligned}&\{\boldsymbol{S}'_{f,4-\mathrm{DoF}}\}_{\text{Derived I}}\\&=\boldsymbol{t}_c\begin{pmatrix}0\\ \boldsymbol{s}_c\end{pmatrix}\Delta 2\tan\frac{\theta_{13}}{2}\begin{pmatrix}\boldsymbol{s}_1\\ \boldsymbol{r}_{13}\times\boldsymbol{s}_1\end{pmatrix}\\&\quad\times\Delta 2\tan\frac{\theta_{12}}{2}\begin{pmatrix}\boldsymbol{s}_1\\ \boldsymbol{r}_{12}\times\boldsymbol{s}_1\end{pmatrix}\Delta 2\tan\frac{\theta_{11}}{2}\begin{pmatrix}\boldsymbol{s}_1\\ \boldsymbol{r}_{11}\times\boldsymbol{s}_1\end{pmatrix}\end{aligned} \tag{11}$$

After the replacement in the standard Type I configuration using this method, it includes three R joints with parallel axes. Through the synthesis algorithm of the finite screw, three factors of R can be rewritten to obtain two circle translations and one rotation as in (12).

$$\begin{aligned}&\{\boldsymbol{S}'_{f,4-\mathrm{DoF}}\}_{\text{Derived I}}\\&=\boldsymbol{t}_c\begin{pmatrix}0\\ \boldsymbol{s}_c\end{pmatrix}\\&\quad\times\Delta\begin{pmatrix}0\\ (\exp(-\theta_{13}\tilde{\boldsymbol{s}}_1)-\exp(-\theta_1\tilde{\boldsymbol{s}}_1))(\boldsymbol{r}_{13}-\boldsymbol{r}_{12})\end{pmatrix}\\&\quad\times\Delta\begin{pmatrix}0\\ \left(\exp\left(-\sum_{i=2}^{3}\theta_{1i}\tilde{\boldsymbol{s}}_1\right)-\exp(-\theta_1\tilde{\boldsymbol{s}}_1)\right)(\boldsymbol{r}_{12}-\boldsymbol{r}_{11})\end{pmatrix}\\&\quad\times\Delta 2\tan\frac{\sum_{i=1}^{3}\theta_{1i}}{2}\begin{pmatrix}\boldsymbol{s}_1\\ \boldsymbol{r}_{13}\times\boldsymbol{s}_1\end{pmatrix}\end{aligned} \tag{12}$$

When the two variables in the above equation are transformed by (13), it has two circle translations with a radius of $|\boldsymbol{r}_1-\boldsymbol{r}_{12}|$ and $|\boldsymbol{r}_{12}-\boldsymbol{r}_{11}|$, respectively, which are equivalent to (6) when the radius tend to infinity and $\boldsymbol{s}_1^{\mathrm{T}}\boldsymbol{s}_c\neq 0$.

$$\sum_{i=1}^{3}\theta_{1i}\mapsto\theta_1,\boldsymbol{r}_{13}\mapsto\boldsymbol{r}_1 \tag{13}$$

Two feasible equivalent derived type I structures with 4-DoF were obtained by equivalent transformation of joints in Standard Type I. The translation and rotation factors in $R_1R_1P_bP_c$ and $R_1R_1R_1P_c$ of Derived Type I and Standard Type I were changed position using the screw triangle product rule to obtain Extended Type I, which are: $P_aR_1P_bP_c$, $P_aP_bR_1P_c$, $P_aP_bP_cR_1$, $R_1P_bR_1P_c$, $P_bR_1R_1P_c$, $R_1P_bP_cR_1$, $P_bR_1P_cR_1$, $P_bP_cR_1R_1$, $R_1R_1P_cR_1$, $R_1P_cR_1R_1$, $P_cR_1R_1R_1$.Taking the $R_1P_bP_cR_1$ as an example, it is characterized as follows:

$$\begin{aligned}\{\boldsymbol{S}'_{f,4-\mathrm{DoF}}\}_{\text{Expand I}}&=2\tan\frac{\theta_{12}}{2}\begin{pmatrix}\boldsymbol{s}_1\\ \boldsymbol{r}_{12}\times\boldsymbol{s}_1\end{pmatrix}\Delta\boldsymbol{t}_b\begin{pmatrix}0\\ \boldsymbol{s}_b\end{pmatrix}\\&\quad\times\Delta\boldsymbol{t}_c\begin{pmatrix}0\\ \boldsymbol{s}_c\end{pmatrix}\Delta 2\tan\frac{\theta_{11}}{2}\begin{pmatrix}\boldsymbol{s}_1\\ \boldsymbol{r}_{11}\times\boldsymbol{s}_1\end{pmatrix}\end{aligned} \tag{14}$$

The translation and rotation factors in (14) can be transformed screw triangle product rule, and combined with the R factors with parallel axes through synthesis algorithm. Equation (14) can be rewritten as:

$$\begin{aligned}&\{\boldsymbol{S}'_{f,4-\mathrm{DoF}}\}_{\text{Expand I}}\\&=\boldsymbol{t}_b\begin{pmatrix}0\\ \exp(-\theta_{12}\tilde{\boldsymbol{s}}_1)\boldsymbol{s}_b\end{pmatrix}\Delta\boldsymbol{t}_c\begin{pmatrix}0\\ \exp(-\theta_{12}\tilde{\boldsymbol{s}}_1)\boldsymbol{s}_c\end{pmatrix}\\&\quad\times\Delta\begin{pmatrix}0\\ (\exp(-\theta_{12}\tilde{\boldsymbol{s}}_1)-\exp(-\theta_1\tilde{\boldsymbol{s}}_1))(\boldsymbol{r}_1-\boldsymbol{r}_{11})\end{pmatrix}\\&\quad\times\Delta 2\tan\frac{\theta_1}{2}\begin{pmatrix}\boldsymbol{s}_1\\ \boldsymbol{r}_1\times\boldsymbol{s}_1\end{pmatrix}\end{aligned} \tag{15}$$

When the radius of circle translation tends to infinity, i.e., $|\boldsymbol{r}_1-\boldsymbol{r}_{11}|\to\infty$, it is equivalent to (6). Similarly, these ten Extended type I structures $P_aR_1P_bP_c$, $P_aP_bR_1P_c$, $P_aP_bP_cR_1$, $R_1P_bR_1P_c$, $P_bR_1R_1P_c$, $P_bR_1P_cR_1$, $P_bP_cR_1R_1$, $R_1R_1P_cR_1$, $R_1P_cR_1R_1$, $P_cR_1R_1R_1$ are also equivalent to (6) and are all feasible. All equivalent and feasible derived type I and extended type I structures were obtained through equivalent transformation or change position of joints of the standard type I, as shown in Fig. 5.

IV. DERIVED AND EXPANDED TYPES OF THE STANDARD TYPE II CONFIGURATION

A. DERIVED TYPE I OF 5-DOF

The standard Type II is a 5-DoF limb. By performing equivalent transformations of the joints in the standard Type II, the 5-DOF derived Type I can be obtained. Four approaches are adopted, with the first approach involving the replacement of one P joint in the standard Type I configuration, i.e., $R_1P_a\mapsto R_1R_1$ or $R_2R_2\mapsto R_1P_a$, resulting in the transformation of the standard Type II configuration into $R_1R_2R_2P_bP_c$ or $R_1R_1R_2P_bP_c$. The second approach involves replacing two P joints in the standard Type II with two R joints whose axes are not parallel, i.e., $P_aP_b\mapsto R_1R_2$, resulting in the transformation of the standard Type II configuration into $R_1R_1R_2R_2P_c$. The third approach involves replacing two P joints in the standard Type II with two R joints whose axes are parallel, i.e., $P_aP_b\mapsto R_1R_1$ or $P_aP_b\mapsto R_2R_2$, resulting in the transformation of the standard Type II configuration into $R_1R_1R_1R_2P_c$ or $R_1R_2R_2R_2P_c$. The fourth involves replacing three P joints in the standard Type II, i.e., $P_aP_bP_c\mapsto R_1R_1R_2$ or $P_aP_bP_c\mapsto R_1R_2R_2$, resulting in the transformation of the standard Type II configuration into $R_1R_1R_1R_2R_2$ or $R_1R_1R_2R_2R_2$.

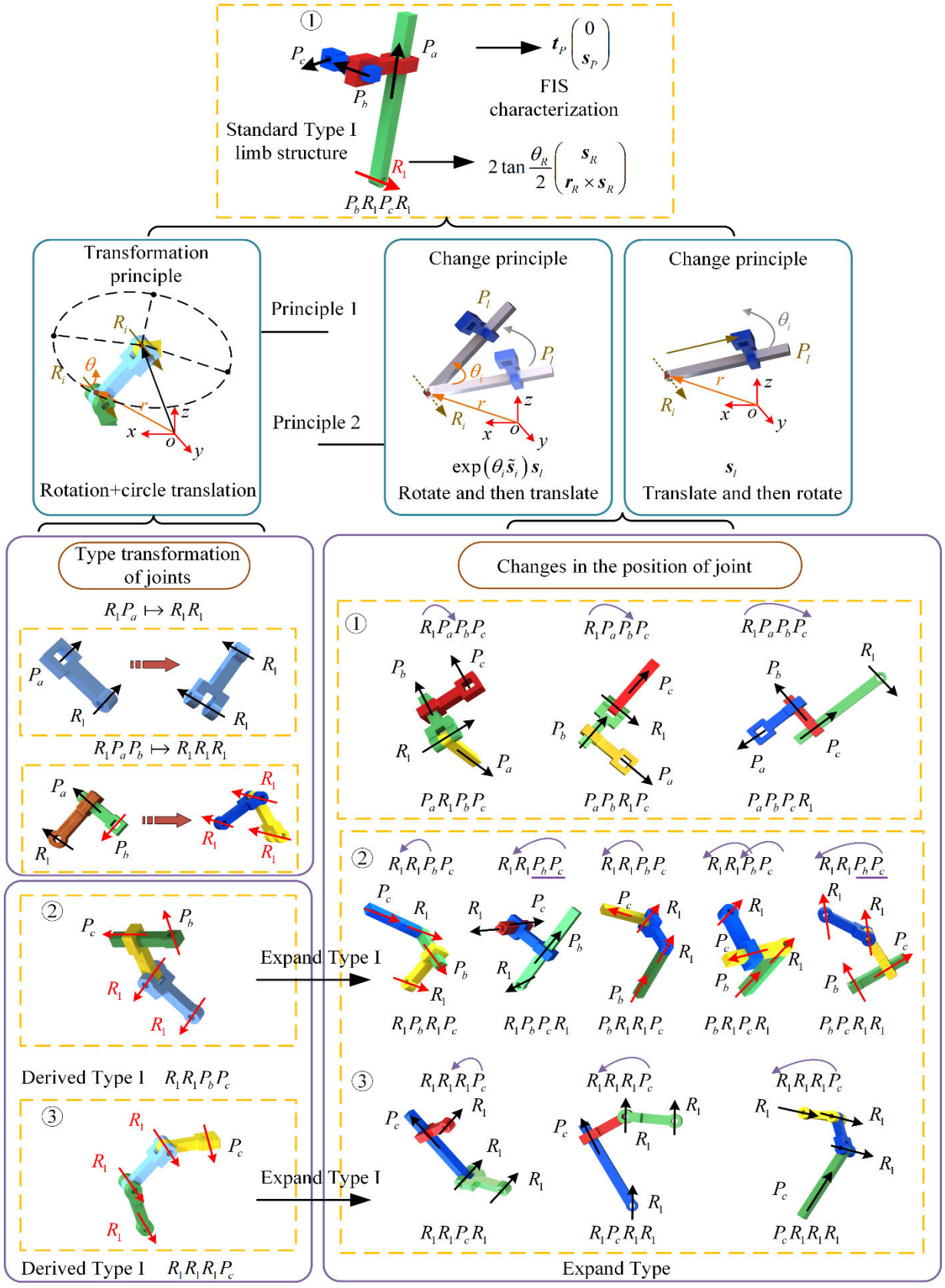

FIGURE 5. All feasible derivative limb structures of 4-DoF.

TABLE 1. Limb structure of derived type I.

Standard Type II	Derived Type I
$R_1R_2P_aP_bP_c$ (3T2R)	$R_1R_2R_2P_bP_c$, $R_1R_1R_2P_bP_c$, $R_1R_1R_2R_2P_c$, $R_1R_1R_1R_2P_c$, $R_1R_2R_2R_2P_c$, $R_1R_1R_1R_2R_2$, $R_1R_1R_2R_2R_2$

Through the aforementioned four approaches, the standard Type II has been derived into seven different Derived Type I configurations.

Taking the $R_1R_2R_2P_bP_c$ structure from the first approach as an example, it is characterized as:

$$\begin{aligned}&\{\boldsymbol{S}'_{f,5-\mathrm{DoF}}\}_{\text{Derived I}}\\&=\boldsymbol{t}_c\begin{pmatrix}0\\\boldsymbol{s}_c\end{pmatrix}\Delta\boldsymbol{t}_b\begin{pmatrix}0\\\boldsymbol{s}_b\end{pmatrix}\Delta2\tan\frac{\theta_{22}}{2}\begin{pmatrix}\boldsymbol{s}_2\\\boldsymbol{r}_{22}\times\boldsymbol{s}_2\end{pmatrix}\\&\quad\times\Delta2\tan\frac{\theta_{21}}{2}\begin{pmatrix}\boldsymbol{s}_2\\\boldsymbol{r}_{21}\times\boldsymbol{s}_2\end{pmatrix}\Delta2\tan\frac{\theta_1}{2}\begin{pmatrix}\boldsymbol{s}_1\\\boldsymbol{r}_1\times\boldsymbol{s}_1\end{pmatrix}\end{aligned}\tag{16}$$

The structure factors include three R joints, with two of the joint axes being parallel. Through the synthesis algorithm of finite screw, the factors can be rewritten as in (17). Verify its feasibility with the specific process outlined in Fig. 6.

$$\begin{aligned}&\{\boldsymbol{S}'_{f,5-\mathrm{DoF}}\}_{\text{Derived I}}\\&=\boldsymbol{t}_c\begin{pmatrix}0\\\boldsymbol{s}_c\end{pmatrix}\Delta\boldsymbol{t}_b\begin{pmatrix}0\\\boldsymbol{s}_b\end{pmatrix}\\&\quad\times\Delta\begin{pmatrix}0\\(\exp(-\theta_{22}\tilde{\boldsymbol{s}}_2)-\exp(-\theta_2\tilde{\boldsymbol{s}}_2))(\boldsymbol{r}_2-\boldsymbol{r}_{11})\end{pmatrix}\\&\quad\times\Delta2\tan\frac{\theta_2}{2}\begin{pmatrix}\boldsymbol{s}_2\\\boldsymbol{r}_2\times\boldsymbol{s}_2\end{pmatrix}\Delta2\tan\frac{\theta_1}{2}\begin{pmatrix}\boldsymbol{s}_1\\\boldsymbol{r}_1\times\boldsymbol{s}_1\end{pmatrix}\end{aligned}\tag{17}$$

When the radius of circle translation tends to infinity, i.e., $|\boldsymbol{r}_2-\boldsymbol{r}_{11}|\to\infty$ and $\boldsymbol{s}_2\times(\boldsymbol{s}_b\times\boldsymbol{s}_c)\neq0$, it is equivalent to (7). Similarly, the other six structures are equivalent to (7) and all are feasible. All equivalent and feasible Derived Type I structures were derived through the equivalent joint transformations of the standard Type II, as shown in Table 1.

B. EXPANDED TYPE I OF 5-DOF STANDARD AND DERIVED TYPE

Seven feasible equivalent 5-DOF derived Type I structures were obtained by using the Standard Type II. By using the screw triangle product rule to exchange the translation and rotation factors between the Standard Type II and Derived Type I, the Expanded Type can be obtained primarily through two different methods. Method 1 involves fixing the rotation factor and changing the position of the translation factor in the structure to obtain the Expanded Type I. Method 2 involves altering the rotation factor and then changing the position of its translational factor in the structure to obtain the Expanded Type II.

Through Method 1, 39 types of Expanded Type I can be obtained. As an example, the representation of the structure

TABLE 2. Limb structure of expanded type I.

Standard Type II	Derived Type I
$R_1R_2P_aP_bP_c$	$R_1P_aR_2P_bP_c$, $P_aR_1R_2P_bP_c$, $R_1P_aP_bR_2P_c$, $R_1P_aR_2P_bP_c$, $P_aR_1P_bP_cR_2$, $P_aP_bR_1R_2P_c$, $P_aR_1P_bP_cR_2$, $P_aP_bR_1P_cR_2$, $P_aP_bP_cR_1R_2$
$R_1R_2R_2P_bP_c$	$R_1R_2P_bR_2P_c$, $R_1P_bR_2R_2P_c$, $P_bR_1R_2R_2P_c$, $R_1R_2P_bP_cR_2$, $R_1P_bR_2P_cR_2$, $P_bR_1P_cR_2R_2$, $P_bR_1R_2P_cR_2$, $P_bR_1P_cR_2R_2$, $P_bP_cR_1R_2R_2$
$R_1R_1R_2P_bP_c$	$R_1R_1P_bR_2P_c$, $R_1P_bR_1R_2P_c$, $P_bR_1R_1R_2P_c$, $R_1R_1P_bP_cR_2$, $R_1P_bR_1P_cR_2$, $P_bR_1P_cR_1R_2$, $P_bR_1R_1P_cR_2$, $P_bR_1P_cR_1R_2$, $P_bP_cR_1R_1R_2$
$R_1R_1R_2R_2P_c$	$R_1R_1R_2P_cR_2$, $R_1R_1P_cR_2R_2$, $R_1P_cR_1R_2R_2$, $P_cR_1R_1R_2R_2$
$R_1R_1R_1R_2P_c$	$R_1R_1R_1P_cR_2$, $R_1R_1P_cR_1R_2$, $R_1P_cR_1R_1R_2$, $P_cR_1R_1R_1R_2$
$R_1R_2R_2R_2P_c$	$R_1R_2R_2P_cR_2$, $R_1R_2P_cR_2R_2$, $R_1P_cR_2R_2R_2$, $P_cR_1R_2R_2R_2$
$R_1R_1R_1R_2R_2$	none
$R_1R_1R_2R_2R_2$	

$R_1P_aR_2P_bP_c$ transformed from the Derived Type I is as follows:

$$\begin{aligned}&\{\boldsymbol{S}'_{f,5-\mathrm{DoF}}\}_{\text{Expand I}}\\&=\boldsymbol{t}_c\begin{pmatrix}0\\\boldsymbol{s}_c\end{pmatrix}\Delta\boldsymbol{t}_b\begin{pmatrix}0\\\boldsymbol{s}_b\end{pmatrix}\Delta2\tan\frac{\theta_2}{2}\begin{pmatrix}\boldsymbol{s}_2\\\boldsymbol{r}_2\times\boldsymbol{s}_2\end{pmatrix}\\&\quad\times\Delta\boldsymbol{t}_a\begin{pmatrix}0\\\boldsymbol{s}_a\end{pmatrix}\Delta2\tan\frac{\theta_1}{2}\begin{pmatrix}\boldsymbol{s}_1\\\boldsymbol{r}_1\times\boldsymbol{s}_1\end{pmatrix}\end{aligned}\tag{18}$$

The axes of the two R factors in the structure are not parallel, so the synthesis algorithm cannot be used. The P factor and R factor can be operated using the properties of the screw triangle product, and then the (18) can be rewritten using the linearity property of the P factor as:

$$\begin{aligned}&\{\boldsymbol{S}'_{f,5-\mathrm{DoF}}\}_{\text{Expand I}}\\&=\boldsymbol{t}_c\begin{pmatrix}0\\\exp(-\theta_1\tilde{\boldsymbol{s}}_1)\exp(-\theta_2\tilde{\boldsymbol{s}}_2)\boldsymbol{s}_c\end{pmatrix}\\&\quad\times\Delta\boldsymbol{t}_b\begin{pmatrix}0\\\exp(-\theta_1\tilde{\boldsymbol{s}}_1)\exp(-\theta_2\tilde{\boldsymbol{s}}_2)\boldsymbol{s}_b\end{pmatrix}\\&\quad\Delta\boldsymbol{t}_a\begin{pmatrix}0\\\exp(-\theta_1\tilde{\boldsymbol{s}}_1)\boldsymbol{s}_a\end{pmatrix}\\&\quad\times\Delta2\tan\frac{\theta_1}{2}\begin{pmatrix}\boldsymbol{s}_1\\\boldsymbol{r}_1\times\boldsymbol{s}_1\end{pmatrix}\Delta2\tan\frac{\theta_2}{2}\begin{pmatrix}\boldsymbol{s}_2\\\boldsymbol{r}_2\times\boldsymbol{s}_2\end{pmatrix}\end{aligned}\tag{19}$$

Equation (19) contains three translation factors and two rotation factors with non-parallel axes, which is equivalent to equation (7).

Similarly, the other 38 types of Expanded Type I can be rewritten using the properties of the screw triangle product, which are equivalent to (7) and are feasible, and will not be further elaborated here.

By displacing the translational and rotational factors of the standard Type II and the derived Type I structures, all equivalent feasible Expanded Type I structures have been derived as shown in Table 2.

C. EXPANDED TYPE II OF 5-DOF STANDARD AND DERIVED TYPE

Through Method 2, one can modify the relative positions of the rotation factors in the derived Type I structure and then change the positions of its translation factors within the structure to obtain the Expanded Type II. When constructing the limb structure, the specific axis orientation of the joint is not distinguished. Therefore, among the seven feasible equivalent structures, $R_1R_2R_2P_bP_c/R_1R_1R_2P_bP_c$, $R_1R_1R_1R_2P_c/R_1R_2R_2R_2P_c$ and $R_1R_1R_1R_2R_2/R_1R_1R_2R_2R_2$ are considered as the same limb structure. The seven feasible equivalent structures can be reclassified into five as shown in the first column of Table 3.

First, by changing the relative positions of the rotation factors in these five structures, new structure can be obtained. One new structure can be obtained from $R_1R_2R_2P_bP_c/R_1R_1R_2P_bP_c$ as $R_1R_2R_1P_bP_c$, two new structures can be obtained from $R_1R_1R_1R_2P_c/R_1R_2R_2R_2P_c$ as $R_1R_1R_2R_1P_c$ and $R_1R_2R_1P_1P_c$, and two new structures can be obtained from $R_1R_1R_2R_2P_c$ as $R_1R_2R_2R_1P_c$ and $R_1R_2R_1R_2P_c$.

Furthermore, by displacing the translation factors in the aforementioned new structures, a total of 41 extended Type II structures can be obtained. There are 9 extended Type II structures derived from $R_1R_2R_1P_bP_c$. Taking $R_1R_2P_bP_cR_1$ as an example for analysis, it is characterized as:

$$\begin{aligned}&\left\{\boldsymbol{S}'_{f,5-\mathrm{DoF}}\right\}_{\text{Expand II}}\\&=2\tan\frac{\theta_{11}}{2}\begin{pmatrix}\boldsymbol{s}_1\\\boldsymbol{r}_{11}\times\boldsymbol{s}_1\end{pmatrix}\Delta 2\tan\frac{\theta_2}{2}\begin{pmatrix}\boldsymbol{s}_2\\\boldsymbol{r}_2\times\boldsymbol{s}_2\end{pmatrix}\\&\quad\times\Delta\boldsymbol{t}_b\begin{pmatrix}0\\\boldsymbol{s}_b\end{pmatrix}\Delta\boldsymbol{t}_c\begin{pmatrix}0\\\boldsymbol{s}_c\end{pmatrix}\Delta 2\tan\frac{\theta_{12}}{2}\begin{pmatrix}\boldsymbol{s}_1\\\boldsymbol{r}_{12}\times\boldsymbol{s}_1\end{pmatrix}\end{aligned}\tag{20}$$

Using the property of screw triangle product, rewrite the (20) as:

$$\begin{aligned}&\left\{\boldsymbol{S}'_{f,5-\mathrm{DoF}}\right\}_{\text{Expand II}}\\&=\boldsymbol{t}_c\begin{pmatrix}0\\\exp\left(-\theta_{12}\tilde{\boldsymbol{s}}_1\right)\exp\left(-\theta_2\tilde{\boldsymbol{s}}_2\right)\boldsymbol{s}_c\end{pmatrix}\\&\quad\times\Delta\boldsymbol{t}_b\begin{pmatrix}0\\\exp\left(-\theta_{12}\tilde{\boldsymbol{s}}_1\right)\exp\left(-\theta_2\tilde{\boldsymbol{s}}_2\right)\boldsymbol{s}_b\end{pmatrix}\\&\quad\times\Delta\begin{pmatrix}0\\\left(\exp\left(-\theta_{12}\tilde{\boldsymbol{s}}_1\right)-\exp\left(-\theta_1\tilde{\boldsymbol{s}}_1\right)\right)\left(\boldsymbol{r}_1-\boldsymbol{r}_{11}\right)\end{pmatrix}\\&\quad\times\Delta 2\tan\frac{\theta_1}{2}\begin{pmatrix}\boldsymbol{s}_1\\\boldsymbol{r}_1\times\boldsymbol{s}_1\end{pmatrix}\\&\quad\times\Delta 2\tan\frac{\theta_2}{2}\\&\quad\times\begin{pmatrix}\exp\left(\theta_{11}\tilde{\boldsymbol{s}}_1\right)\boldsymbol{s}_2\\\left(\boldsymbol{r}_{11}+\exp\left(\theta_2\tilde{\boldsymbol{s}}_2\right)\left(\boldsymbol{r}_{11}-\boldsymbol{r}_2\right)\right)\times\left(\exp\left(\theta_2\tilde{\boldsymbol{s}}_2\right)\boldsymbol{s}_1\right)\end{pmatrix}\end{aligned}\tag{21}$$

Equation (21) only contains two R factors with different axes, which is not equivalent to (7), but it satisfies the conditions of $\left\{\boldsymbol{S}_{f,Standard2}\right\}\subseteq\left\{\boldsymbol{S}'_{f,5-\mathrm{DoF}}\right\}_{\text{Expand II}}$. Although the structure is not equivalent to the standard Type II, it is a viable structure. Similarly, the other 8 extended Type II structures derived from it are also non-equivalent but feasible limb structures, which will not be elaborated on here.

There are a total of 8 types of extended type II derived from $R_1R_1R_2P_1P_c$ and $R_1R_2R_1P_1P_c$. Taking $R_1R_1R_2P_cR_1$ and $R_1R_2R_1P_cR_1$ as examples for analysis, $R_1R_1R_2P_cR_1$ characterized as:

$$\begin{aligned}&\left\{\boldsymbol{S}'_{f,5-\mathrm{DoF}}\right\}_{\text{Expand II}}\\&=2\tan\frac{\theta_{11}}{2}\begin{pmatrix}\boldsymbol{s}_1\\\boldsymbol{r}_{11}\times\boldsymbol{s}_1\end{pmatrix}\Delta 2\tan\frac{\theta_{12}}{2}\begin{pmatrix}\boldsymbol{s}_1\\\boldsymbol{r}_{12}\times\boldsymbol{s}_1\end{pmatrix}\\&\quad\times\Delta 2\tan\frac{\theta_2}{2}\begin{pmatrix}\boldsymbol{s}_2\\\boldsymbol{r}_2\times\boldsymbol{s}_2\end{pmatrix}\Delta\boldsymbol{t}_c\begin{pmatrix}0\\\boldsymbol{s}_c\end{pmatrix}\\&\quad\times\Delta 2\tan\frac{\theta_{13}}{2}\begin{pmatrix}\boldsymbol{s}_1\\\boldsymbol{r}_{13}\times\boldsymbol{s}_1\end{pmatrix}\end{aligned}\tag{22}$$

Using the property of screw triangle product, rewrite the (22) as:

$$\begin{aligned}&\left\{\boldsymbol{S}'_{f,5-\mathrm{DoF}}\right\}_{\text{Expand II}}\\&=\begin{pmatrix}0\\\left(\exp\left(-\theta_{11}\tilde{\boldsymbol{s}}_1\right)-\exp\left(-\theta_1\tilde{\boldsymbol{s}}_1\right)\right)\left(\boldsymbol{r}_1-\boldsymbol{r}_{12}\right)\end{pmatrix}\\&\quad\times\Delta\boldsymbol{t}_c\begin{pmatrix}0\\\exp\left(-\theta_1\tilde{\boldsymbol{s}}_1\right)\exp\left(-\theta_2\tilde{\boldsymbol{s}}_2\right)\boldsymbol{s}_c\end{pmatrix}\\&\quad\times\Delta\begin{pmatrix}0\\\left(\exp\left(-\theta_1\tilde{\boldsymbol{s}}_1\right)-\exp\left(-\left(\theta_1+\theta_{13}\right)\tilde{\boldsymbol{s}}_1\right)\right)\left(\boldsymbol{r}_1-\boldsymbol{r}_{13}\right)\end{pmatrix}\\&\quad\times\Delta 2\tan\frac{\theta_1}{2}\begin{pmatrix}\boldsymbol{s}_1\\\boldsymbol{r}_1\times\boldsymbol{s}_1\end{pmatrix}\\&\quad\times\Delta 2\tan\frac{\theta_2}{2}\\&\quad\times\begin{pmatrix}\exp\left(\theta_{13}\tilde{\boldsymbol{s}}_1\right)\boldsymbol{s}_2\\\left(\boldsymbol{r}_{13}+\exp\left(\theta_{13}\tilde{\boldsymbol{s}}_1\right)\left(\boldsymbol{r}_2-\boldsymbol{r}_{13}\right)\right)\times\left(\exp\left(\theta_{13}\tilde{\boldsymbol{s}}_1\right)\boldsymbol{s}_2\right)\end{pmatrix}\end{aligned}\tag{23}$$

Equation (23) is not equivalent to (7), but it meets the condition of $\left\{\boldsymbol{S}_{f,Standard2}\right\}\subseteq\left\{\boldsymbol{S}'_{f,5-\mathrm{DoF}}\right\}_{\text{Expand II}}$. Although the structure is not equivalent to the standard Type II, it is a feasible structure.

$R_1R_2R_1P_cR_1$ characterized as:

$$\begin{aligned}&\left\{\boldsymbol{S}'_{f,5-\mathrm{DoF}}\right\}_{\text{Expand II}}\\&=2\tan\frac{\theta_{11}}{2}\begin{pmatrix}\boldsymbol{s}_1\\\boldsymbol{r}_{11}\times\boldsymbol{s}_1\end{pmatrix}\Delta 2\tan\frac{\theta_2}{2}\begin{pmatrix}\boldsymbol{s}_2\\\boldsymbol{r}_2\times\boldsymbol{s}_2\end{pmatrix}\\&\quad\times\Delta 2\tan\frac{\theta_{12}}{2}\begin{pmatrix}\boldsymbol{s}_1\\\boldsymbol{r}_{12}\times\boldsymbol{s}_1\end{pmatrix}\Delta\boldsymbol{t}_c\begin{pmatrix}0\\\boldsymbol{s}_c\end{pmatrix}\\&\quad\times\Delta 2\tan\frac{\theta_{13}}{2}\begin{pmatrix}\boldsymbol{s}_1\\\boldsymbol{r}_{13}\times\boldsymbol{s}_1\end{pmatrix}\end{aligned}\tag{24}$$

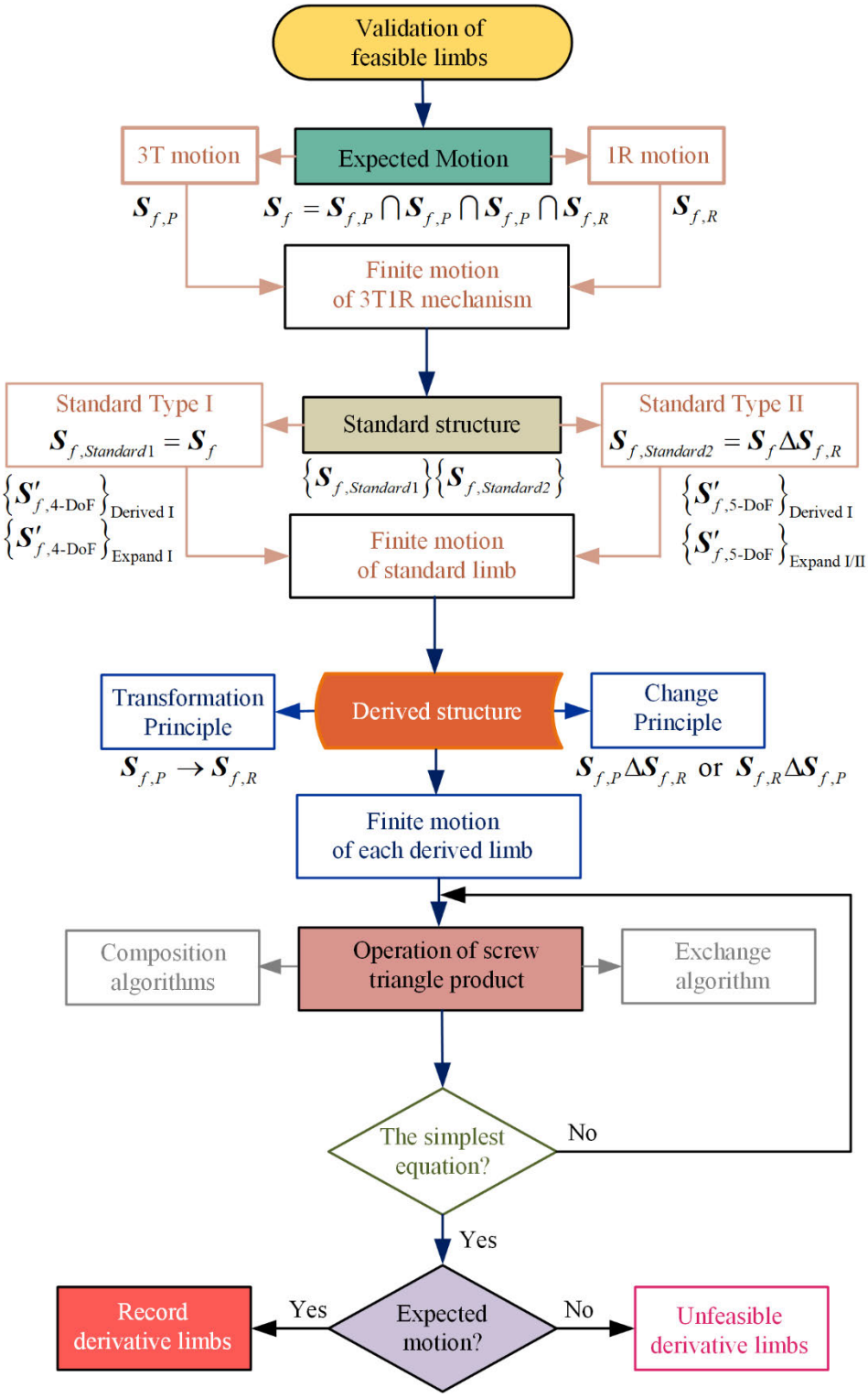

FIGURE 6. Feasibility verification flowchart of limb structure.

Using the property of screw triangle product, rewrite the (24) as:

$$\{S'_{f,5-\text{DoF}}\}_{\text{Expand II}} = \begin{pmatrix} 0 \\ (\exp(-\theta_{11}\tilde{s}_1) - \exp(-\theta_1\tilde{s}_1))(r_1 - r_{12}) \end{pmatrix} \times \Delta 2 \tan\frac{\theta_1}{2}\begin{pmatrix} s_1 \\ r_1 \times s_1 \end{pmatrix}$$

$$\times \Delta 2\tan\frac{\theta_2}{2} \times \begin{pmatrix} \exp(\theta_{12}\tilde{\boldsymbol{s}}_1)\,\boldsymbol{s}_2 \\ (\boldsymbol{r}_{12}+\exp(\theta_{12}\tilde{\boldsymbol{s}}_1)(\boldsymbol{r}_2-\boldsymbol{r}_{12}))\times(\exp(\theta_{12}\tilde{\boldsymbol{s}}_1)\,\boldsymbol{s}_2) \end{pmatrix} \times \Delta t_c \begin{pmatrix} 0 \\ \boldsymbol{s}_c \end{pmatrix} \Delta 2\tan\frac{\theta_{13}}{2}\begin{pmatrix} \boldsymbol{s}_1 \\ \boldsymbol{r}_{13}\times\boldsymbol{s}_1 \end{pmatrix} \tag{25}$$

Equation (24) is not equivalent to (7), but it meets the condition of $\{\boldsymbol{S}_{f,Standard2}\} \subseteq \{\boldsymbol{S}'_{f,5-\mathrm{DoF}}\}_{\text{Expand II}}$.it is a feasible structure. Similarly, the other six types of extended Type II derived from these two structures are also non-equivalent feasible limb structures, which will not be elaborated here.

There are a total of 8 types of extended type II derived from $R_1R_2R_2R_1P_c$ and $R_1R_2R_1R_2P_c$. Taking $R_1R_2R_2P_cR_1$ and $R_1R_2R_1R_2P_c$ as examples for analysis, $R_1R_2R_2P_cR_1$ characterized as:

$$\begin{aligned} &\{\boldsymbol{S}'_{f,5-\mathrm{DoF}}\}_{\text{Expand II}} \\ &= 2\tan\frac{\theta_{11}}{2}\begin{pmatrix} \boldsymbol{s}_1 \\ \boldsymbol{r}_{11}\times\boldsymbol{s}_1 \end{pmatrix} \Delta 2\tan\frac{\theta_{21}}{2}\begin{pmatrix} \boldsymbol{s}_2 \\ \boldsymbol{r}_{21}\times\boldsymbol{s}_2 \end{pmatrix} \\ &\quad\times \Delta 2\tan\frac{\theta_{22}}{2}\begin{pmatrix} \boldsymbol{s}_2 \\ \boldsymbol{r}_{22}\times\boldsymbol{s}_2 \end{pmatrix} \Delta t_c \begin{pmatrix} 0 \\ \boldsymbol{s}_c \end{pmatrix} \\ &\quad\times \Delta 2\tan\frac{\theta_{12}}{2}\begin{pmatrix} \boldsymbol{s}_1 \\ \boldsymbol{r}_{12}\times\boldsymbol{s}_1 \end{pmatrix} \end{aligned} \tag{26}$$

Using the property of screw triangle product, rewrite the (26) as:

$$\begin{aligned} &\{\boldsymbol{S}'_{f,5-\mathrm{DoF}}\}_{\text{Expand II}} \\ &= \begin{pmatrix} 0 \\ (\exp(-\theta_{22}\tilde{\boldsymbol{s}}_2)-\boldsymbol{E}_3)(\boldsymbol{r}_2-\boldsymbol{r}_{22}) \end{pmatrix} \\ &\quad\times \Delta t_c \begin{pmatrix} 0 \\ \exp(-\theta_{11}\tilde{\boldsymbol{s}}_1)\exp(-\theta_2\tilde{\boldsymbol{s}}_2)\,\boldsymbol{s}_c \end{pmatrix} \\ &\quad\times \Delta \begin{pmatrix} 0 \\ (\exp(-\theta_{11}\tilde{\boldsymbol{s}}_1)-\exp(-\theta_1\tilde{\boldsymbol{s}}_1))(\boldsymbol{r}_1-\boldsymbol{r}_{12}) \end{pmatrix} \\ &\quad\times \Delta 2\tan\frac{\theta_1}{2}\begin{pmatrix} \boldsymbol{s}_1 \\ \boldsymbol{r}_1\times\boldsymbol{s}_1 \end{pmatrix} \\ &\quad\times \Delta 2\tan\frac{\theta_2}{2} \\ &\quad\times \begin{pmatrix} \exp(\theta_{12}\tilde{\boldsymbol{s}}_1)\,\boldsymbol{s}_2 \\ (\boldsymbol{r}_{12}+\exp(\theta_{12}\tilde{\boldsymbol{s}}_1)(\boldsymbol{r}_2-\boldsymbol{r}_{12}))\times(\exp(\theta_{12}\tilde{\boldsymbol{s}}_1)\,\boldsymbol{s}_2) \end{pmatrix} \end{aligned} \tag{27}$$

Equation (27) is not equivalent to (7), but it meets the condition of $\{\boldsymbol{S}_{f,Standard2}\} \subseteq \{\boldsymbol{S}'_{f,5-\mathrm{DoF}}\}_{\text{Expand II}}$.it is a feasible structure. Similarly, The other three types of $R_1R_2P_cR_2R_1$, $R_1P_cR_2R_2R_1$, and $P_cR_1R_2R_2R_1$ derived from $R_1R_2R_2R_1P_c$ are also non-equivalent feasible structures, which will not be elaborated here.

$P_cR_1R_2R_1R_2$ characterized as:

$$\begin{aligned} &\{\boldsymbol{S}'_{f,5-\mathrm{DoF}}\}_{\text{Expand II}} \\ &= \boldsymbol{t}_c\begin{pmatrix} 0 \\ \boldsymbol{s}_c \end{pmatrix} \Delta 2\tan\frac{\theta_{11}}{2}\begin{pmatrix} \boldsymbol{s}_1 \\ \boldsymbol{r}_{11}\times\boldsymbol{s}_1 \end{pmatrix} \\ &\quad \Delta 2\tan\frac{\theta_{21}}{2}\begin{pmatrix} \boldsymbol{s}_2 \\ \boldsymbol{r}_{21}\times\boldsymbol{s}_2 \end{pmatrix} \Delta 2\tan\frac{\theta_{12}}{2}\begin{pmatrix} \boldsymbol{s}_1 \\ \boldsymbol{r}_{12}\times\boldsymbol{s}_1 \end{pmatrix} \\ &\quad\times \Delta 2\tan\frac{\theta_{22}}{2}\begin{pmatrix} \boldsymbol{s}_2 \\ \boldsymbol{r}_{22}\times\boldsymbol{s}_2 \end{pmatrix} \end{aligned} \tag{28}$$

Using the property of screw triangle product, rewrite the (28) as:

$$\begin{aligned} &\{\boldsymbol{S}'_{f,5-\mathrm{DoF}}\}_{\text{Expand II}} \\ &= \boldsymbol{t}_c\begin{pmatrix} 0 \\ \boldsymbol{s}_c \end{pmatrix} \\ &\quad\times \Delta \begin{pmatrix} 0 \\ (\exp(-\theta_{12}\tilde{\boldsymbol{s}}_1)-\exp(-\theta_1\tilde{\boldsymbol{s}}_{11}))(\boldsymbol{r}_1-\boldsymbol{r}_{11}) \end{pmatrix} \\ &\quad\times \Delta 2\tan\frac{\theta_1}{2}\begin{pmatrix} \boldsymbol{s}_1 \\ \boldsymbol{r}_1\times\boldsymbol{s}_1 \end{pmatrix} \\ &\quad\times \Delta 2\tan\frac{\theta_{22}}{2} \\ &\quad\times \begin{pmatrix} \exp(\theta_{11}\tilde{\boldsymbol{s}}_1)\,\boldsymbol{s}_2 \\ (\boldsymbol{r}_{11}+\exp(\theta_1\tilde{\boldsymbol{s}}_1)(\boldsymbol{r}_{22}-\boldsymbol{r}_{11}))\times(\exp(\theta_{11}\tilde{\boldsymbol{s}}_1)\,\boldsymbol{s}_2) \end{pmatrix} \\ &\quad\times \Delta 2\tan\frac{\theta_{21}}{2}\begin{pmatrix} \boldsymbol{s}_2 \\ \boldsymbol{r}_{21}\times\boldsymbol{s}_2 \end{pmatrix} \end{aligned} \tag{29}$$

Equation (29) only contains two translation factors and three rotation factors with different axes, which do not meet the expected motion of the mechanism. Therefore, the structure is unfeasible. Similarly, The other three types of $R_1R_2R_1P_cR_2$, $R_1R_2P_cR_1R_2$, and $R_1P_cR_2R_1R_2$ derived from $R_1R_2R_1R_2P_c$ are also unfeasible structures, which will not be elaborated here.

There are a total of 8 types of extended type II derived from $R_1R_1R_1R_2R_2$ and $R_1R_1R_2R_2R_2$, namely $R_1R_2R_2R_2R_1$, $R_1R_2R_2R_1R_1$, $R_1R_1R_2R_2R_1$, $R_1R_2R_1R_2R_1$, $R_1R_2R_1R_2R_2$, $R_1R_1R_2R_1R_2$, $R_1R_2R_1R_1R_2$, $R_1R_2R_2R_1R_2$. Taking $R_1R_2R_2R_2R_1$ and $R_1R_2R_1R_2R_2$ as examples for analysis, $R_1R_2R_2R_2R_1$ characterized as:

$$\begin{aligned} &\{\boldsymbol{S}'_{f,5-\mathrm{DoF}}\}_{\text{Expand II}} \\ &= 2\tan\frac{\theta_{11}}{2}\begin{pmatrix} \boldsymbol{s}_1 \\ \boldsymbol{r}_{11}\times\boldsymbol{s}_1 \end{pmatrix} \Delta 2\tan\frac{\theta_{21}}{2}\begin{pmatrix} \boldsymbol{s}_2 \\ \boldsymbol{r}_{21}\times\boldsymbol{s}_2 \end{pmatrix} \\ &\quad\times \Delta 2\tan\frac{\theta_{22}}{2}\begin{pmatrix} \boldsymbol{s}_2 \\ \boldsymbol{r}_{22}\times\boldsymbol{s}_2 \end{pmatrix} \Delta 2\tan\frac{\theta_{23}}{2}\begin{pmatrix} \boldsymbol{s}_2 \\ \boldsymbol{r}_{23}\times\boldsymbol{s}_2 \end{pmatrix} \\ &\quad\times \Delta 2\tan\frac{\theta_{12}}{2}\begin{pmatrix} \boldsymbol{s}_1 \\ \boldsymbol{r}_{12}\times\boldsymbol{s}_1 \end{pmatrix} \end{aligned} \tag{30}$$

Using the property of screw triangle product, rewrite the (30) as (31), shown at the bottom of the next page.

Equation (31) contains three circle translations, the first two of which have radius of $|\boldsymbol{r}_{21}-\boldsymbol{r}_2|$ and $|\boldsymbol{r}_2-\boldsymbol{r}_{23}|$, respectively, and are perpendicular to $\exp(-\theta_{11}\tilde{\boldsymbol{s}}_1)\,\boldsymbol{s}_2$, while the third has a radius of $|\boldsymbol{r}_1-\boldsymbol{r}_{12}|$ and is perpendicular to $\exp(-\theta_{11}\tilde{\boldsymbol{s}}_1)\,\boldsymbol{s}_2$. While $|\boldsymbol{r}_{21}-\boldsymbol{r}_2|\to\infty$ and $|\boldsymbol{r}_{21}-\boldsymbol{r}_2|\to\infty$, it is not equivalent to (7), but it meets the expected motion of the mechanism, so it is feasible. Similarly, $R_1R_1R_2R_2R_1$ and $R_1R_2R_2R_1R_1$ are also feasible structures.

$R_1R_2R_1R_2R_2$ characterized as:

$$\begin{aligned} &\{\boldsymbol{S}'_{f,5-\mathrm{DoF}}\}_{\text{Expand II}} \\ &= 2\tan\frac{\theta_{11}}{2}\begin{pmatrix} \boldsymbol{s}_1 \\ \boldsymbol{r}_{11}\times\boldsymbol{s}_1 \end{pmatrix} \Delta 2\tan\frac{\theta_{21}}{2}\begin{pmatrix} \boldsymbol{s}_2 \\ \boldsymbol{r}_{21}\times\boldsymbol{s}_2 \end{pmatrix} \end{aligned}$$

$$\times \Delta 2\tan\frac{\theta_{12}}{2}\begin{pmatrix}\boldsymbol{s}_1\\ \boldsymbol{r}_{12}\times\boldsymbol{s}_1\end{pmatrix}\Delta 2\tan\frac{\theta_{22}}{2}\begin{pmatrix}\boldsymbol{s}_2\\ \boldsymbol{r}_{22}\times\boldsymbol{s}_2\end{pmatrix}$$
$$\times \Delta 2\tan\frac{\theta_{23}}{2}\begin{pmatrix}\boldsymbol{s}_2\\ \boldsymbol{r}_{23}\times\boldsymbol{s}_2\end{pmatrix} \tag{32}$$

Using the property of screw triangle product, rewrite the (32) as:

$$\begin{aligned}&\{\boldsymbol{S'}_{f,5-\mathrm{DoF}}\}_{\text{Expand II}}\\ &=\begin{pmatrix}0\\ (\exp(-\theta_{11}\tilde{s}_1)-\exp(-\theta_1\tilde{s}_1))(\boldsymbol{r}_1-\boldsymbol{r}_{12})\end{pmatrix}\\ &\quad\times\Delta 2\tan\frac{\theta_1}{2}\begin{pmatrix}\boldsymbol{s}_1\\ \boldsymbol{r}_1\times\boldsymbol{s}_1\end{pmatrix}\\ &\quad\times\Delta 2\tan\frac{\theta_{21}}{2}\\ &\quad\times\begin{pmatrix}\exp(\theta_{12}\tilde{s}_1)\boldsymbol{s}_2\\ (\boldsymbol{r}_{12}+\exp(\theta_{12}\tilde{s}_1)(\boldsymbol{r}_{21}-\boldsymbol{r}_{12}))\times(\exp(\theta_{12}\tilde{s}_1)\boldsymbol{s}_2)\end{pmatrix}\\ &\quad\times\Delta\begin{pmatrix}0\\ (\exp(-\theta_{22}\tilde{s}_2)-\exp(-\theta_2\tilde{s}_2))(\boldsymbol{r}_2-\boldsymbol{r}_{23})\end{pmatrix}\\ &\quad\times\Delta 2\tan\frac{\theta_2}{2}\begin{pmatrix}\boldsymbol{s}_2\\ \boldsymbol{r}_2\times\boldsymbol{s}_2\end{pmatrix}\end{aligned} \tag{33}$$

Equation (33) only contains two translation factors and three rotation factors with different axes, which do not meet the expected motion of the mechanism. Therefore, the structure is unfeasible. Similarly, The other four types of $R_1R_2R_1R_2R_1$, $R_1R_1R_2R_1R_2$, $R_1R_2R_1R_1R_2$ and $R_1R_2R_2R_1R_2$ are also unfeasible structures, which will not be elaborated here.

In summary, among the 41 extended Type II structures derived, 13 structures are deemed infeasible, not meeting the expected motion requirements of the parallel positioning mechanism. All equivalent feasible or non-equivalent feasible extended Type II structures are shown in Table 3.

TABLE 3. Limb structure of expanded type II.

Standard Type II	Change position	Extended Type II
$R_1R_2P_aP_bP_c$	none	none
$R_1R_2R_2P_bP_c$ / $R_1R_1R_2P_bP_c$	$R_1R_2R_1P_bP_c$	$R_1R_2P_bP_cR_1$, $R_1P_bP_cR_2R_1$, $P_bP_cR_1R_2R_1$, $R_1R_2P_bR_1P_c$, $R_1P_bR_2R_1P_c$, $P_bR_1R_2R_1P_c$, $R_1P_bR_2P_cR_1$, $P_bR_1R_2P_cR_1$, $P_bR_1P_cR_2R_1$
$R_1R_1R_1P_2P_c$ / $R_1R_2R_2P_2P_c$	$R_1R_1R_2P_1P_c$ $R_1R_2R_1R_1P_c$	$R_1R_1R_2P_cR_1$, $R_1R_1P_cR_2R_1$, $R_1P_cR_1R_2R_1$, $P_cR_1R_1R_2R_1$, $R_1R_2R_1P_cR_1$, $R_1R_2P_cR_1R_1$, $P_cR_1R_2R_1R_1$
$R_1R_1R_2R_2P_c$	$R_1R_2R_2R_1P_c$	$R_1R_2R_2P_cR_1$, $R_1R_2P_cR_2R_1$, $R_1P_cR_2R_2R_1$, $P_cR_1R_2R_2R_1$
$R_1R_1R_1R_2R_2$ / $R_1R_1R_2R_2R_2$	none	$R_1R_2R_2R_2R_1$, $R_1R_1R_2R_2R_1$, $R_1R_2R_2R_1R_1$

V. UNITS ASSEMBLY CONDITIONS AND CONFIGURATION SELECTION

Based on the desired motion, a total of 14 4-DOF and 71 5-DOF limb structures have been derived from the standard Type I and Type II structures. These limb structures are capable of achieving the required 3T1R motion for grinding operations. The finite motion of 3T can be represented by (34). When selecting a limb structure for assembly, the distribution of joint axes should be considered. When the directions of the R_1 and R_2 axes in the feasible limb structure are consistent with $\boldsymbol{s}_1$, the finite motion can be represented by (35).

$$\boldsymbol{S}_{f,P}=\boldsymbol{t}_c\begin{pmatrix}0\\ \boldsymbol{s}_c\end{pmatrix}\Delta\boldsymbol{t}_b\begin{pmatrix}0\\ \boldsymbol{s}_b\end{pmatrix}\Delta\boldsymbol{t}_a\begin{pmatrix}0\\ \boldsymbol{s}_a\end{pmatrix} \tag{34}$$

$$\{\boldsymbol{S}_f\}=\boldsymbol{S}_{f,P}\Delta 2\tan\frac{\theta_1}{2}\begin{pmatrix}\boldsymbol{s}_1\\ \boldsymbol{r}\times\boldsymbol{s}_1\end{pmatrix} \tag{35}$$

The R_1 and R_2 joints rotate in the directions of $\boldsymbol{s}_1$ and $\boldsymbol{s}_2$ respectively. The first case is that the mechanism rotates around direction $\boldsymbol{s}_1$ to reach the singularity position, and then changes to rotate around direction $\boldsymbol{s}_2$, as shown in (36).

The second case is that the mechanism rotates around direction $\boldsymbol{s}_2$ to reach the singularity position, and then changes to rotate around direction $\boldsymbol{s}_1$, as shown in (37). The third case is that the mechanism starts rotating around the $\boldsymbol{s}_1$ and $\boldsymbol{s}_2$ directions from the singularity position, as shown in (38).

$$\{\boldsymbol{S}_f\}=\left\{\boldsymbol{S}_{f,P}\Delta 2\tan\frac{\theta_1}{2}\begin{pmatrix}\boldsymbol{s}_1\\ \boldsymbol{r}\times\boldsymbol{s}_1\end{pmatrix}\right\}$$

$$\begin{aligned}\{\boldsymbol{S'}_{f,5-\mathrm{DoF}}\}_{\text{Expand II}}&=\begin{pmatrix}0\\ \exp(-\theta_{11}\tilde{s}_1)(\exp(-\theta_{21}\tilde{s}_2)-\exp(-\theta_2\tilde{s}_2))(\boldsymbol{r}_{21}-\boldsymbol{r}_2)\end{pmatrix}\\ &\quad\times\Delta\begin{pmatrix}0\\ \exp(-\theta_{11}\tilde{s}_1)(\exp(-(\theta_{21}+\theta_{22})\tilde{s}_2)-\exp(-\theta_2\tilde{s}_2))(\boldsymbol{r}_2-\boldsymbol{r}_{23})\end{pmatrix}\\ &\quad\times\Delta\begin{pmatrix}0\\ (\exp(-\theta_{11}\tilde{s}_1)-\exp(-\theta_1\tilde{s}_1))(\boldsymbol{r}_1-\boldsymbol{r}_{12})\end{pmatrix}\Delta 2\tan\frac{\theta_1}{2}\begin{pmatrix}\boldsymbol{s}_1\\ \boldsymbol{r}_1\times\boldsymbol{s}_1\end{pmatrix}\\ &\quad\times\Delta 2\tan\frac{\theta_{21}}{2}\begin{pmatrix}\exp(\theta_{12}\tilde{s}_1)\boldsymbol{s}_2\\ (\boldsymbol{r}_{12}+\exp(\theta_{12}\tilde{s}_1)(\boldsymbol{r}_{21}-\boldsymbol{r}_{12}))\times(\exp(\theta_{12}\tilde{s}_1)\boldsymbol{s}_2)\end{pmatrix}\end{aligned} \tag{31}$$

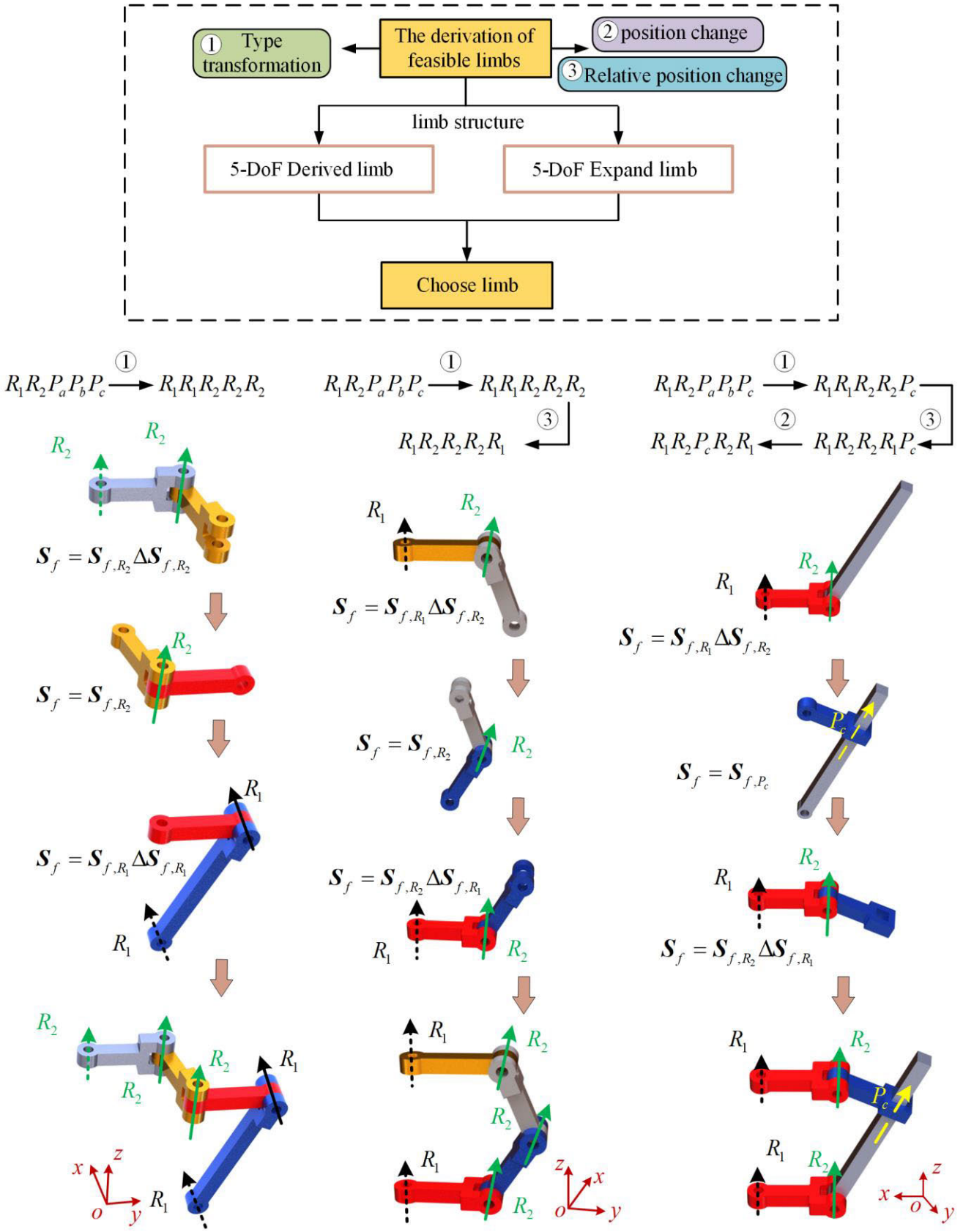

FIGURE 7. Selected three limb structures.

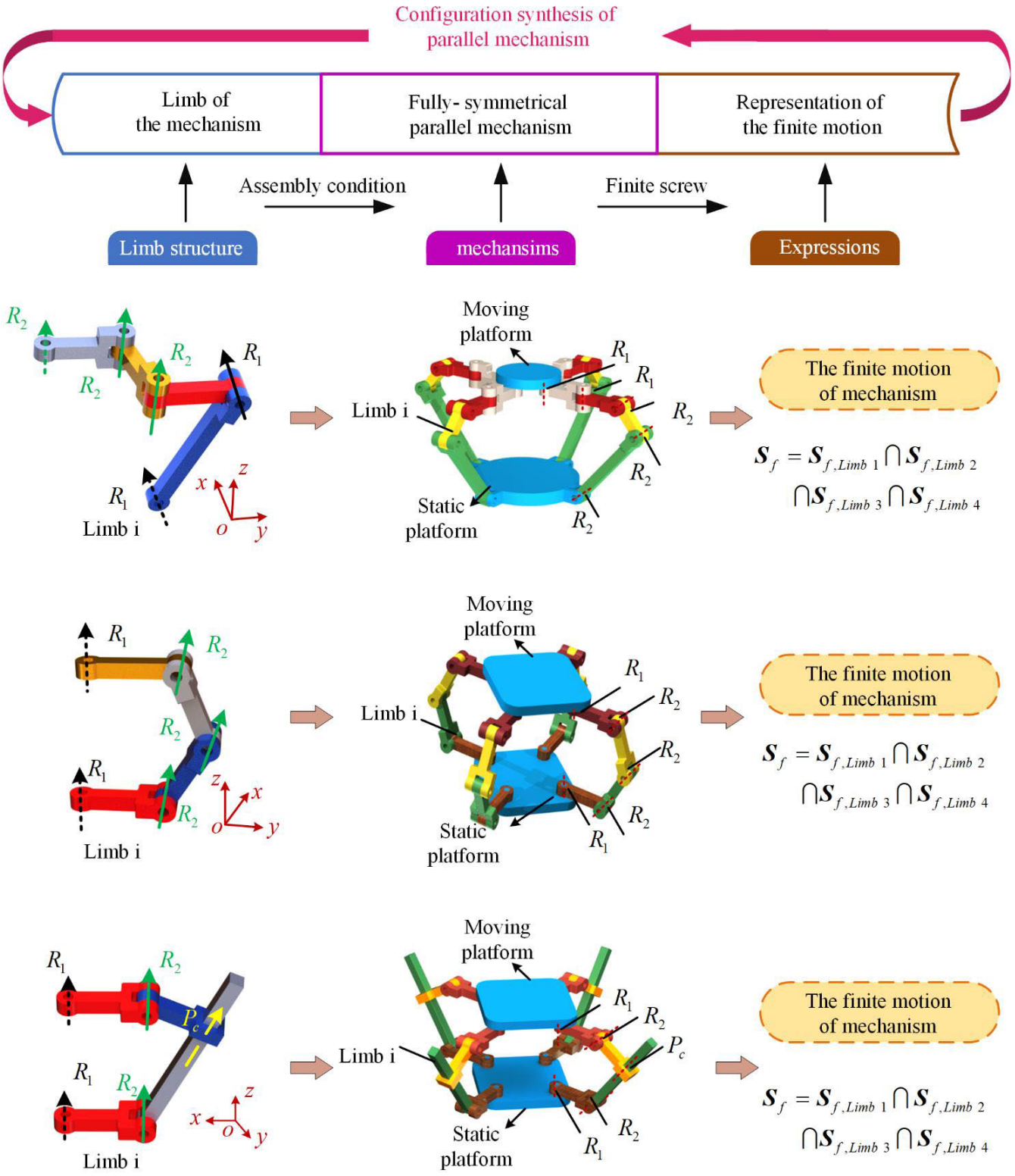

FIGURE 8. Configurations of three fully symmetrical parallel mechanism.

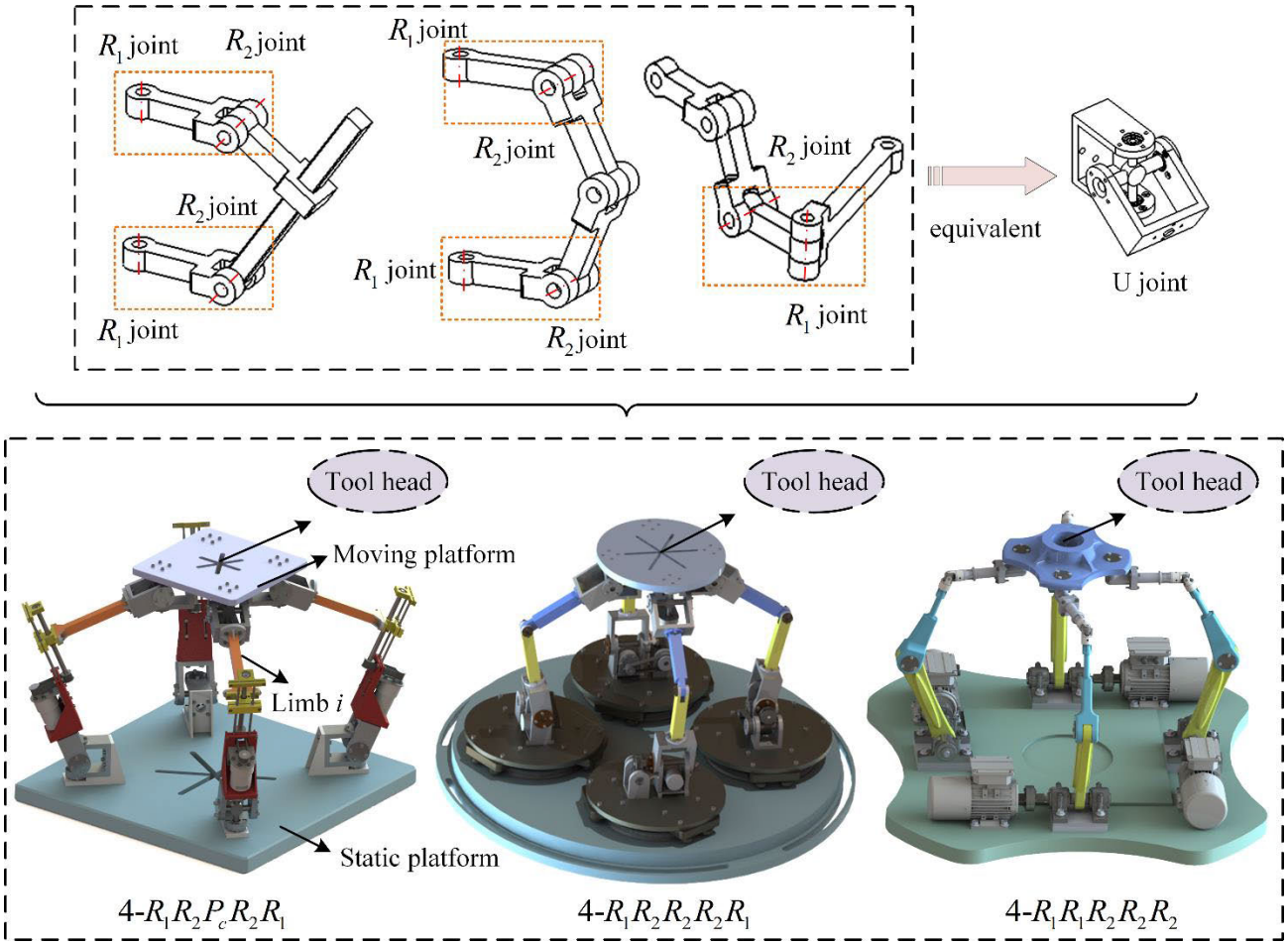

FIGURE 9. Virtual prototype.

$$\cup \left\{ \boldsymbol{S}_{f,P} \Delta 2 \tan \frac{\theta_1'}{2} \begin{pmatrix} \boldsymbol{s}_1 \\ \boldsymbol{r} \times \boldsymbol{s}_1 \end{pmatrix} \Delta 2 \tan \frac{\theta_2}{2} \begin{pmatrix} \boldsymbol{s}_2 \\ \boldsymbol{r} \times \boldsymbol{s}_2 \end{pmatrix} \right\} \tag{36}$$

where θ_1' is the angle at which the mechanism rotates in the direction of $\boldsymbol{s}_1$ to a singular configuration.

$$\{\boldsymbol{S}_f\} = \left\{ \boldsymbol{S}_{f,P} \Delta 2 \tan \frac{\theta_2}{2} \begin{pmatrix} \boldsymbol{s}_2 \\ \boldsymbol{r} \times \boldsymbol{s}_2 \end{pmatrix} \right\} \cup \left\{ \boldsymbol{S}_{f,P} \Delta 2 \tan \frac{\theta_2'}{2} \begin{pmatrix} \boldsymbol{s}_2 \\ \boldsymbol{r} \times \boldsymbol{s}_2 \end{pmatrix} \Delta 2 \tan \frac{\theta_1}{2} \begin{pmatrix} \boldsymbol{s}_1 \\ \boldsymbol{r} \times \boldsymbol{s}_1 \end{pmatrix} \right\} \tag{37}$$

$$\{\boldsymbol{S}_f\} = \left\{ \boldsymbol{S}_{f,P} \Delta 2 \tan \frac{\theta_1}{2} \begin{pmatrix} \boldsymbol{s}_1 \\ \boldsymbol{r} \times \boldsymbol{s}_1 \end{pmatrix} \right\} \cup \left\{ \boldsymbol{S}_{f,P} \Delta 2 \tan \frac{\theta_2}{2} \begin{pmatrix} \boldsymbol{s}_2 \\ \boldsymbol{r} \times \boldsymbol{s}_2 \end{pmatrix} \right\} \tag{38}$$

The finite motion of the mechanism's moving platform can be represented by the intersection of each limb. Avoid additional rotation during intersection operations, as the axis directions of the R joints between each limb are not the same. To ensure that there is no degree of freedom in which the axis direction changes with the rotation angle under intersection operations. When the selected limb has 5-DoF, it is also required that the number of limbs be greater than or equal to three. Selecting any three types of limb structures from the table of feasible 5-DoF limb structures as examples, the configuration is shown in Fig. 7. Considering the requirement for the mechanism to be fully symmetrical and the number of limbs to be no less than three, taking into account the stiffness and precise positioning needs during the grinding process, a configuration with four limbs is adopted. Each limb is distributed at 90 degrees relative to the moving platform, as illustrated in Fig. 8.

The limb structure selected for configuration 1 is $R_1R_1R_2R_2R_2$, and the finite motion of its single limb can be expressed as:

$$\begin{aligned} \boldsymbol{S}_{f,i} = {} & 2 \tan \frac{\theta_{i,5}}{2} \begin{pmatrix} \boldsymbol{s}_{i,5} \\ \boldsymbol{r}_{i,5} \times \boldsymbol{s}_{i,5} \end{pmatrix} \Delta 2 \tan \frac{\theta_{i,4}}{2} \begin{pmatrix} \boldsymbol{s}_{i,4} \\ \boldsymbol{r}_{i,4} \times \boldsymbol{s}_{i,4} \end{pmatrix} \\ & \times \Delta 2 \tan \frac{\theta_{i,3}}{2} \begin{pmatrix} \exp\left(\theta_{i,4} \tilde{\boldsymbol{s}}_{i,4}\right) \boldsymbol{s}_{i,3} \\ \boldsymbol{r}_{i,4} \times \exp\left(\theta_{i,4} \tilde{\boldsymbol{s}}_{i,4}\right) \boldsymbol{s}_{i,3} \end{pmatrix} \\ & \times \Delta 2 \tan \frac{\theta_{i,2}}{2} \begin{pmatrix} \boldsymbol{s}_{i,2} \\ \boldsymbol{r}_{i,2} \times \boldsymbol{s}_{i,2} \end{pmatrix} \Delta 2 \tan \frac{\theta_{i,1}}{2} \begin{pmatrix} \boldsymbol{s}_{i,1} \\ \boldsymbol{r}_{i,1} \times \boldsymbol{s}_{i,1} \end{pmatrix} \end{aligned} \tag{39}$$

The finite motion of the entire mechanism can be represented as:

$$\boldsymbol{S}_f = \boldsymbol{S}_{f,1} \cap \boldsymbol{S}_{f,2} \cap \boldsymbol{S}_{f,3} \cap \boldsymbol{S}_{f,4} \tag{40}$$

The limb structure selected for configuration 2 is $R_1R_2R_2R_2R_1$, and the finite motion of its single limb can be expressed as:

$$\begin{aligned}\boldsymbol{S}_{f,i} = {} & 2\tan\frac{\theta_{i,5}}{2}\begin{pmatrix}\boldsymbol{s}_{i,5}\\ \boldsymbol{r}_{i,5}\times\boldsymbol{s}_{i,5}\end{pmatrix}\\ & \times\Delta 2\tan\frac{\theta_{i,4}}{2}\begin{pmatrix}\exp\left(\theta_{i,5}\tilde{\boldsymbol{s}}_{i,5}\right)\boldsymbol{s}_{i,4}\\ \boldsymbol{r}_{i,5}\times\exp\left(\theta_{i,5}\tilde{\boldsymbol{s}}_{i,5}\right)\boldsymbol{s}_{i,4}\end{pmatrix}\\ & \times\Delta 2\tan\frac{\theta_{i,3}}{2}\begin{pmatrix}\boldsymbol{s}_{i,3}\\ \boldsymbol{r}_{i,3}\times\boldsymbol{s}_{i,3}\end{pmatrix}\Delta 2\tan\frac{\theta_{i,2}}{2}\begin{pmatrix}\boldsymbol{s}_{i,2}\\ \boldsymbol{r}_{i,2}\times\boldsymbol{s}_{i,2}\end{pmatrix}\\ & \times\Delta 2\tan\frac{\theta_{i,1}}{2}\begin{pmatrix}\exp\left(\theta_{i,2}\tilde{\boldsymbol{s}}_{i,2}\right)\boldsymbol{s}_{i,1}\\ \boldsymbol{r}_{i,2}\times\exp\left(\theta_{i,2}\tilde{\boldsymbol{s}}_{i,2}\right)\boldsymbol{s}_{i,1}\end{pmatrix}\end{aligned} \tag{41}$$

The finite motion of the entire mechanism can be represented as:

$$\boldsymbol{S}_f = \boldsymbol{S}_{f,1} \cap \boldsymbol{S}_{f,2} \cap \boldsymbol{S}_{f,3} \cap \boldsymbol{S}_{f,4} \tag{42}$$

The limb structure selected for configuration 3 is $R_1R_2P_cR_2R_1$, and the finite motion of its single limb can be expressed as:

$$\begin{aligned}\boldsymbol{S}_{f,i} = {} & 2\tan\frac{\theta_{i,5}}{2}\begin{pmatrix}\boldsymbol{s}_{i,5}\\ \boldsymbol{r}_{i,5}\times\boldsymbol{s}_{i,5}\end{pmatrix}\\ & \times\Delta 2\tan\frac{\theta_{i,4}}{2}\begin{pmatrix}\exp\left(\theta_{i,5}\tilde{\boldsymbol{s}}_{i,5}\right)\boldsymbol{s}_{i,4}\\ \boldsymbol{r}_{i,5}\times\exp\left(\theta_{i,5}\tilde{\boldsymbol{s}}_{i,5}\right)\boldsymbol{s}_{i,4}\end{pmatrix}\\ & \times\Delta\boldsymbol{t}_3\begin{pmatrix}0\\ \boldsymbol{s}_3\end{pmatrix}\Delta 2\tan\frac{\theta_{i,2}}{2}\begin{pmatrix}\boldsymbol{s}_{i,2}\\ \boldsymbol{r}_{i,2}\times\boldsymbol{s}_{i,2}\end{pmatrix}\\ & \times\Delta 2\tan\frac{\theta_{i,1}}{2}\begin{pmatrix}\exp\left(\theta_{i,2}\tilde{\boldsymbol{s}}_{i,2}\right)\boldsymbol{s}_{i,1}\\ \boldsymbol{r}_{i,2}\times\exp\left(\theta_{i,2}\tilde{\boldsymbol{s}}_{i,2}\right)\boldsymbol{s}_{i,1}\end{pmatrix}\end{aligned} \tag{43}$$

The finite motion of the entire mechanism can be represented as:

$$\boldsymbol{S}_f = \boldsymbol{S}_{f,1} \cap \boldsymbol{S}_{f,2} \cap \boldsymbol{S}_{f,3} \cap \boldsymbol{S}_{f,4} \tag{44}$$

Considering the large number of motion joints and connecting rods in the above three configurations, the overall stiffness of the mechanism will be affected. Therefore, two adjacent R joints in each limb that satisfy the vertical relationship of the axis are equivalent to U joints, which simplifies the limb structure, reduces the number of connecting rods, and improves the overall stiffness of the mechanism. The virtual prototypes of the three configurations are shown in Fig. 9.

VI. CONCLUSION

For the grinding operation of large structural components, a fully symmetrical parallel positioning mechanism is adopted to achieve the machining operation.

(1) Based on finite screw for configuration synthesis, the desired motion of the mechanism is determined through the movements involved in grinding operations.

(2) From the desired motions, standard Type I and Type II configurations are derived, further leading to 85 feasible limb structures of 4-DoF and 5-DoF.

(3) Three limb structures were selected from 85 types of limb structures. Taking these three limb structures as examples, three fully-symmetrical parallel positioning mechanisms were configured as in-situ grinding processing mechanisms based on assembly conditions and requirements of positioning accuracy and machining stiffness.

REFERENCES

[1] H. Chen, J. Yang, and H. Ding, "Robotic compliant grinding of curved parts based on a designed active force-controlled end-effector with optimized series elastic component," *Robot. Comput.-Integr. Manuf.*, vol. 86, Apr. 2024, Art. no. 102646.
[2] J. Li, L. Zou, G. Luo, W. Wang, and C. Lv, "Enhancement and evaluation in path accuracy of industrial robot for complex surface grinding," *Robot. Comput.-Integr. Manuf.*, vol. 81, Jun. 2023, Art. no. 102521.
[3] Q. Wang, W. Wang, X. Ding, and C. Yun, "A force control joint for robot–environment contact application," *J. Mech. Robot.*, vol. 11, no. 3, Jun. 2019, Art. no. 034502.
[4] F. Guo, G. Cheng, and Y. Pang, "Explicit dynamic modeling with joint friction and coupling analysis of a 5-DOF hybrid polishing robot," *Mechanism Mach. Theory*, vol. 167, Jan. 2022, Art. no. 104509.
[5] Y. M. Feng, Z. Guo, P. F. Wang, T. Sun, and B. B. Lian, "Synthesis of configuration for a class of hybrid flexible mechanisms with shaft-hole assembly," *Trans. Tianjin Univ.*, vol. 53, no. 6, pp. 582–592, 2020.
[6] L. Xu, X. Chai, and Y. Ding, "Design of a 2RRU-RRS parallel kinematic mechanism for an inner-cavity machining hybrid robot," *J. Mech. Robot.*, vol. 16, no. 5, May 2024, Art. no. 054501.
[7] X. Fugui, M. Bin, L. Xinjun, Z. Jiabo, and Y. Yi, "Novel mode and equipment for machining large complex components," *J. Mech. Eng.*, vol. 56, no. 19, p. 70, 2020.
[8] A. Olarra, D. Axinte, L. Uriarte, and R. Bueno, "Machining with the WalkingHex: A walking parallel kinematic machine tool for in situ operations," *CIRP Ann.*, vol. 66, no. 1, pp. 361–364, 2017.
[9] K. Chen, M. Wang, X. Huo, P. Wang, and T. Sun, "Topology and dimension synchronous optimization design of 5-DoF parallel robots for in-situ machining of large-scale steel components," *Mechanism Mach. Theory*, vol. 179, Jan. 2023, Art. no. 105105.
[10] X. Kong and C. M. Gosselin, "Type synthesis of 3T1R 4-DOF parallel manipulators based on screw theory," *IEEE Trans. Robot. Autom.*, vol. 20, no. 2, pp. 181–190, Apr. 2004.
[11] O. Salgado, O. Altuzarra, V. Petuya, and A. Hernández, "Synthesis and design of a novel 3T1R fully-parallel manipulator," *J. Mech. Des.*, vol. 130, no. 4, Apr. 2008, Art. no. 042305.
[12] Y. Wu, H. Wang, and Z. Li, "Quotient kinematics machines: Concept, analysis, and synthesis," *J. Mech. Robot.*, vol. 3, no. 4, Nov. 2011, Art. no. 041004.
[13] T. L. Yang, *Topological Structure of Robot Mechanisms*. Beijing, China: Machinery Industry Press, 2004.
[14] T. Sun, S. F. Yang, and B. B. Lian, *Finite and Instantaneous Screw Theory in Robotic Mechanism*. Singapore: Springer, 2020.
[15] T. Sun, S.-F. Yang, T. Huang, and J. S. Dai, "A finite and instantaneous screw based approach for topology design and kinematic analysis of 5-axis parallel kinematic machines," *Chin. J. Mech. Eng.*, vol. 31, no. 1, pp. 31–44, May 2018.
[16] T. Sun and X. Huo, "Type synthesis of 1T2R parallel mechanisms with parasitic motions," *Mechanism Mach. Theory*, vol. 128, pp. 412–428, Oct. 2018.
[17] S. Yang, J. S. Dai, Y. Jin, and R. Fu, "Finite displacement screw-based group analysis of 3PRS parallel mechanisms," *Mechanism Mach. Theory*, vol. 171, May 2022, Art. no. 104727.
[18] S. Yang, T. Sun, T. Huang, Q. Li, and D. Gu, "A finite screw approach to type synthesis of three-DOF translational parallel mechanisms," *Mechanism Mach. Theory*, vol. 104, pp. 405–419, Oct. 2016.
[19] X. Zhao, B. Tao, and H. Ding, "Multimobile robot cluster system for robot machining of large-scale workpieces," *IEEE/ASME Trans. Mechatronics*, vol. 27, no. 1, pp. 561–571, Feb. 2022.
[20] Y. Sun, D. J. Giblin, and K. Kazerounian, "Accurate robotic belt grinding of workpieces with complex geometries using relative calibration techniques," *Robot. Comput.-Integr. Manuf.*, vol. 25, no. 1, pp. 204–210, Feb. 2009.

[21] L. Xu, X. Chai, and Y. Ding, "Design and analysis of a reconfigurable hybrid robot for machining of large workpieces," *J. Mech. Robot.*, vol. 16, no. 5, May 2024, Art. no. 051001.
[22] Y. Wang, Q. Li, and Y. Chen, "Variables increment configuration synthesis method for suspended cable-driven parallel mechanisms," *Mechatronics*, vol. 95, Nov. 2023, Art. no. 103056.
[23] R. Luo, P. Wu, Z. Yu, and Z. Hou, "An overlapped plane model and topology optimization for planar mechanism synthesis," *Comput. Struct.*, vol. 281, Jun. 2023, Art. no. 107019.
[24] T. Tang, H. Fang, H. Luo, Y. Song, and J. Zhang, "Type synthesis, unified kinematic analysis and prototype validation of a family of exechon inspired parallel mechanisms for 5-axis hybrid kinematic machine tools," *Robot. Comput.-Integr. Manuf.*, vol. 72, Dec. 2021, Art. no. 102181.
[25] Y. Kim, H. S. Kim, and T. Seo, "Type synthesis and kinematic analysis of a 2-DOF shape-morphing wheel mechanism for step-overcoming," *IEEE Access*, vol. 9, pp. 86500–86513, 2021.
[26] Y. Wang, F. Yu, Q. Li, and Y. Chen, "Dual-space configuration synthesis method for rigid-flexible coupled cable-driven parallel mechanisms," *Ocean Eng.*, vol. 271, Mar. 2023, Art. no. 113753.
[27] Z. Wang, W. Zhang, and X. Ding, "A family of RCM mechanisms: Type synthesis and kinematics analysis," *Int. J. Mech. Sci.*, vol. 231, Oct. 2022, Art. no. 107590.
[28] X. Hu and H. Liu, "Type synthesis and analysis of a new class of bifurcation 3T2Rv parallel mechanisms with variable/invariable rotational axes," *IEEE Access*, vol. 9, pp. 164300–164315, 2021.
[29] X. Zhao, B. Tao, S. Han, and H. Ding, "Accuracy analysis in mobile robot machining of large-scale workpiece," *Robot. Comput.-Integr. Manuf.*, vol. 71, Oct. 2021, Art. no. 102153.
[30] H.-L. Xie, Q.-H. Wang, S. K. Ong, J.-R. Li, and Z.-P. Chi, "Adaptive human–robot collaboration for robotic grinding of complex workpieces," *CIRP Ann.*, vol. 71, no. 1, pp. 285–288, 2022.
[31] Q. Li and J. M. Hervé, "1T2R parallel mechanisms without parasitic motion," *IEEE Trans. Robot.*, vol. 26, no. 3, pp. 401–410, Jun. 2010.
[32] J. Yu, J. S. Dai, S. Bi, and G. Zong, "Numeration and type synthesis of 3-DOF orthogonal translational parallel manipulators," *Prog. Natural Sci.*, vol. 18, no. 5, pp. 563–574, May 2008.
[33] L. J. Puglisi, R. J. Saltaren, H. A. Moreno, P. F. Cárdenas, C. Garcia, and R. Aracil, "Dimensional synthesis of a spherical parallel manipulator based on the evaluation of global performance indexes," *Robot. Auto. Syst.*, vol. 60, no. 8, pp. 1037–1045, Aug. 2012.
[34] Y. Z. Niu, F. J. Li, J. L. Xu, and S. H. Li, "Configuration synthesis of a three rotational weakly coupled combined mechanism based on inverse Jacobian matrix," *Mach. Tool Hydraulics*, vol. 54, no. 8, pp. 402–410, Aug. 2023.

YANG QI was born in Tianjin, China, in 1988. He received the bachelor's degree in mechanical design manufacturing and automation and the and Ph.D. degree in mechanical engineering from Tianjin University, in 2018.

He is currently an Associate Professor with Tianjin University of Technology and Education. He is the author of 12 patents of innovation and five SCI articles. His research interests include configuration synthesis of parallel mechanisms with complex motion types, integrated design of scale parameters and section parameters for multi performance requirements, flight dynamics in microgravity environment, and the prototype construction of parallel mechanisms.

XINQI TAO was born in Jiangsu, China. She received the bachelor's degree in electronic information engineering from Changshu Institute of Technology, in 2021. She is currently pursuing the master's degree in mechanical engineering with Tianjin University of Technology and Education. She is the author of an EI articles.

XIAOFEI REN was born in Shandong, China. She received the master's degree in education from Tianjin Normal University, in 2016.

She joined Tianjin University of Technology and Education, in March 2017. She has published two articles, participated in the publication of one journal review, and participated in two provincial and ministerial level projects. Her research interest includes mechanical design, with a focus on designing parallel mechanisms with multiple degrees of freedom, which play a crucial role in engineering practice. Through in-depth research on the design and optimization of parallel mechanisms, she is committed to promoting the development and innovation of related technical fields.

HONG WANG was born in Chongqing, China. He received the bachelor's degree in mechanical engineering from Tianjin University of Technology and Education. He is the author of a SCI articles and two EI articles.